University of Stavanger

FACULTY OF SCIENCE AND TECHNOLOGY

MASTER'S THESIS

Study program/specialization: MSc. Petroleum engineering/Natural Gas	Spring semester, 2021 Open access

Author: Fagan Mehdiyev

Faculty supervisor: Professor Steinar Evje

External supervisor: Research Professor Ingebret Fjelde

Title of master's thesis:

Surface Complexation Modelling of Wettability Alteration during Carbonated Water Flooding

Credits: 30 ECTS

Keywords:
Wettability
Surface Complexation Modelling
Carbon Dioxide Flooding
Crude oil/Brine/Rock Interactions
Effective Surface Area
Electrostatic Attraction
Oil Adhesion
Total Bond Product

Number of pages:71

Stavanger, 15th June 2021

Abstract

Within the context of global warming, Carbon Dioxide (CO_2) capture and its utilization in oil recovery are seen as one of the majority methods to decrease Greenhouse Gas (GHG) emissions over the next few decades. CO_2 flooding is considered an Enhanced Oil Recovery (EOR) method and can increase the oil recovery factor up to 60%-70% by changing the wettability preference of the reservoir rock. The aim of this thesis is to estimate the wettability preferences of the individual minerals, reservoir rocks, and mineral mixtures during Formation Water (FW) and Carbonated Water (CW) injection. Moreover, the effects of temperature and pressure on the wettability of an individual mineral (calcite) were also studied to improve the understanding of the CO_2 flooding impact on reservoir rock wettability.

The literature study of this M.Sc. thesis outlines how wettability affects the oil recovery, the impact of the oil composition, brine composition, and CO_2 on the wetting state of the individual minerals and reservoir rock. Moreover, the simulation works were carried out to estimate the wettability preferences of the minerals, Sandstone Reservoir Rocks (SRR), and Pseudo-Sandstone Rock (PSR)/mineral mixtures. The simulation part was based on Surface Complexation Modeling (SCM) and presented a set of simulations in the geochemistry solver PHREEQ-C, run at various pressures and temperatures, in which wettability states were estimated. The wettability preferences were estimated by calculating bond products defined as the product of the mole fraction of oppositely charged oil and mineral surfaces.

During FW injection, SCM results showed that the quartz and albite were strongly hydrophilic while calcite was strongly hydrophobic. On the other hand, clay minerals (i.e., illite and montmorillonite) were less hydrophobic than calcite and more hydrophobic than quartz. In CW, the wettability of dominant (based on weight and surface area) minerals in SRR (i.e., quartz and calcite) was found to be altered toward less hydrophobic, while the opposite effect was noticed for clay minerals. For SRR, the SCM results revealed that their wettability preferences were hydrophilic in both FW and CW. Nonetheless, increasing the content of the hydrophilic minerals increases the rock's tendency to become more hydrophilic.

The SCM results showed that the intrinsic properties of the minerals, such as surface area and surface charge, have an enormous impact on the reservoir rock wetting state. For PSR with low calcite content, the wettability was inclined towards the mineral with dominant surface area. As calcite is strong hydrophobic compared to the other studied minerals, increasing the calcite content altered the wettability of the rock toward less water-wet, even if clay minerals

dominated the effective surface area. From the SCM results, the divalent cations bridging was the dominant oil adsorption mechanism for the main sandstone minerals. Nevertheless, direct adsorption of carboxylate was also estimated in clay minerals and calcite.

In this study, the temperature and pressure effect on the wettability alteration of the calcite was also investigated. However, SCM results at different temperatures and pressures show that these reservoir properties have a minor impact on the wetting state of calcite during FWI and CWI.

The SCM technique is a quick and economical method of estimating the wettability of the minerals and reservoir rocks. SCM can be used as the first screening tool to estimate the potential for CW effect on reservoir wettability. Then further evaluation of potential in laboratory experiments and reservoir simulations should be performed.

As a continuation of the simulation work performed in the present study, it is suggested to perform experiments with FW and CW using the USBM method to determine the wettability preferences of reservoir rocks at various pressures and temperatures. Since the SCM method and flotation tests have limitations in minerals distribution, SCM also has limitations with the effective surface area of minerals. On the other hand, in USBM experiments, mineral distribution can be taken into account. This is because the USBM method estimates the wettability of the bulk rock while the flotation test estimates the wettability of crushed rock.

Acknowledgment

This thesis, “Surface Complexation Modelling of Wettability Alteration during Carbonated Water Flooding” was written during the spring semester of 2021, which was the last step to graduate from an M.Sc. degree in Petroleum Engineering.

I wish to thank the University of Stavanger (UiS) and Norwegian Research Center (NORCE) for giving me a chance to write my M.Sc. thesis on this relevant topic. My special and heartily thanks to my supervisor, Research Professor Ingebret Fjelde, who encouraged and directed me. I would also like to thank Dr. Aruoture Voke Omekeh for his advice throughout the simulation software.

Furthermore, I am thankful to my family and friends for their mental support while working on this thesis.

Table of Contents

List of Figures

List of Tables

Abbreviations

AN	Acidic Number
BP	Bond Product
Ca^{2+}	Calcium Ions
CO_2	Carbon Dioxide
COO^-	Carboxylate
CO_2-WAG	Carbon Dioxide Flooding with WAG
CW	Carbonated Water
CWI	Carbonated Water Injection
EOR	Enhanced Oil Recovery
FW	Formation Water
FWI	Formation Water Injection
GHG	Greenhouse Gas
H^+	Hydrogen Ion
H_2CO_3	Carbonic Acid
H_2O	Water
Mg^{2+}	Magnesium Ion
MMP	Minimum Miscibility Pressure
NCS	Norwegian Continental Shelf
NPC	National Petroleum Council
OOIP	Original Oil in Place
PSR	Pseudo Sandstone Rock, crushed sandstone rock with added minerals
SCM	Surface Complexation Modelling
SRR	Sandstone Reservoir Rock
STO	Stock Tank Oil
TAN	Total Acid Number
TBN	Total Base Number
TBP	Total Bond Product
USBM	United States Bureau of Mines
WAG	Water-Alternating-Gas Process

Nomenclature

ρ_o	Oil density
ρ_w	Water density
θ	Contact angle
θ_D	Dimensionless contact angle
A	Area
A_{eff}	Effective surface area
A_i	Intrinsic surface area of mineral i
E_D	Displacement energy
g	Gravity
h_o	Oil height
h_w	Water height
I_{AH}	Amott-Harvey displacement index
I_o	Oil imbibition index
I_w	Water imbibition index
m_i	Mass fraction of mineral i
Mw	Molecular weight
n_i	Mole fraction of mineral i
O_i	Mole fraction of oil
P	Pressure
r	Pipe radius
T	Temperature
t	CO_2 exposure time
t_D	Dimensionless time
W	Wettability

1 Introduction

1.1 Background

Industrial establishment and its development year by year have increased the energy demand, mainly gained by burning fossil fuels such as coal, oil, and natural gas, also known as hydrocarbons [1]. The combustion of hydrocarbons contributes to Carbon Dioxide (CO2) emission and other Greenhouse Gases (GHG) into the atmosphere. In the right proportion, GHG is necessary for human survival. However, when the concentration of these gases increases in the atmosphere, it leads to the rise of temperatures on our planet. This process is also known as global warming [1].

Over the last half-decade, the main reason for global warming is considered to be human activity. So, all nations' primary objective is to prevent climate change by controlling GHG concentration in the atmosphere [2]. During the manufactural activity, the CO_2 contains the central part of GHG emissions. There are some technological opportunities to reduce CO_2 levels, such as decreasing energy utilization, prioritizing less carbon-intensive fuels, switching to nuclear or alternative energy sources, giving more attention to reforestation processes, and CO_2 capture and storage mechanisms [2].

On the other hand, demand for fossil fuels keeps increasing, so; researches have been carried out to establish new methods to improve the recovery from the reservoirs because hydrocarbons are not renewable sources [3]. Commonly, more than 60% of the Original Oil In Place (OOIP) remains in the reservoir after primary and secondary oil recovery procedures as trapped and bypassed oil [3].

CO_2 flooding is one of the most typical Enhanced Oil Recovery (EOR) methods in the petroleum industry [4]. Moreover, the fundamental reasons for applying this method to oil and gas reservoirs are altering the wettability preferences of the reservoir, reducing oil viscosity, etc., to improve the oil recovery and reduce CO_2 emission. Besides, using CO_2 in EOR is more economically attractive than utilizing other gases [5].

Wettability has been known as one of the essential parameters regulating the remaining oil in place in the reservoir [6]. The information on reservoir wettability is necessary to understand the fluid displacement mechanisms and evolve strategies for accomplishing higher recovery factors.

Different thermal and chemical EOR methods have been investigated to change the reservoir wettability toward water-wetness [7]. The degree of water-wetness that can be accomplished by the EOR method excessively depends on how this method influences Crude Oil/Brine/Rock (COBR) properties. Besides, the process of crude oil interactions with rock and brine for individual oil reservoirs distinctively depends on crude oil and brine composition, rock mineralogy, and other reservoir parameters.

It is commonly concurred that petroleum reservoirs were possessed by water before oil migration at later stages [7]. When oil occupied the porous medium, it did not force out the water entirely because of the water-wet state of the majority of minerals that compose reservoir rock, such as carbonate and silica [8]. Therefore, a thin layer of water has remained covering the rock surface. The water layer exists as a boundary between rock surfaces and oil. The wettability preferences of the reservoir alter when the water layer is destabilized due to oil/water/rock interaction, which may lead to the reservoir becoming oil-wet [9].

Wettability varies for different reservoir rocks. Acidic Number (AN) is the essential factor that controls the wettability alteration of carbonates by crude oil; water-wetness increases as the AN decreases [7]. In sandstones, API, asphaltene content, and clay content are the most important factors of changing the wettability. Therefore, integration of API, AN, clay substance, and asphaltene substance estimation would give important data to assess the composite of mechanisms by which the original wettability of sandstone and limestone is changed to be oil-wet. Thus, this thesis will mainly focus on estimating the wettability of the sandstone reservoir rocks and dominant minerals of these rocks, which further leads to the aim and objectives of this thesis.

1.2 Aim and Objectives

The purpose of the present study is to demonstrate the effect of Carbonated Water Injection (CWI) on the wettability of individual minerals, Sandstone Reservoir Rocks (SRR), and Pseudo-Sandstone Rocks (PSR, crushed sandstone rock with added minerals). This is to improve understanding of the impact of brines (i.e., Formation Water (FW) and Carbonated Water (CW)) and intrinsic parameters on the wettability of the reservoirs. The objectives for the above aim are:

1) To conduct a literature study that will provide a theoretical background for understanding the simulation part of the thesis.

2) To perform SCM simulations by the geochemical solver PHREEQ-C for individual minerals to estimate their wettability preferences. These simulations include:

a) to estimate the wettability state of the individual minerals during FW injection,

b) to estimate the wettability state of the individual minerals during CW injection.

3) To perform SCM simulations by the geochemical solver PHREEQ-C for SRR and PSR to estimate their wettability preferences. These simulations include:

a) to estimate the wettability state of SRR and PSR during FW injection,

b) to estimate the wettability state of SRR and PSR during CW injection.

4) To interpret and compare minerals' and reservoir rocks' (SRR and PSR) wettability state during FW and CW injection.

1.3 Structure of the Thesis

The thesis is organized as follows: first, a literature study is presented in Section 2, which summarises how wettability can be measured, the effect of CO_2 on wettability, and the work that has been previously performed to determine wettability preferences of minerals and reservoir rocks. Following the literature study, Section 3 describes the SCM method and the input parameters for simulations. Section 4 presents the simulation results. These are compared with existing knowledge and previous work on wettability in the discussion in Section 5. Finally, the conclusions are given in Section 6.

2 Literature study

2.1 Wettability

2.1.1 Definition

In a reservoir, the central aspect for controlling the location, flow, and fluid distribution is wettability [10]. Wettability can be defined as tendency of a specific fluid to adhere to a solid surface in the presence of other types of liquids.

One known factor affecting the pore displacement mechanism is the reservoir wetting state [11]. Therefore, knowledge about wettability has an essential role in better understanding multiphase flow problems such as oil migration from a source rock, primary production mechanism, EOR processes, etc. [11].

2.1.2 Classification of Wettability

By the type of wetting fluid, wettability can be divided into three main groups: water-wet, oil-wet, and intermediate (or neutral) wet [8]. When most of the oil/water/rock system surface is wetted by water, it is considered water-wet. At water-wet conditions, the smaller pores and dead-end pores are occupied by water and create a film layer on the mineral surfaces of the larger pores. Moreover, residual oil resides in larger pores as droplets remaining on a water layer. Nevertheless, when the system is preferentially oil-wet, the larger pores are occupied by water, and the rock surface mainly contacts with oil [12].

In a porous medium, one of the fluids (water or oil) acts as a wetting fluid [13]. The description given above for water-wet and oil-wet can be summarized in Figure 2.1. Concerning the intermediate or neutral-wet case, the rock surface has no preference for either fluid.

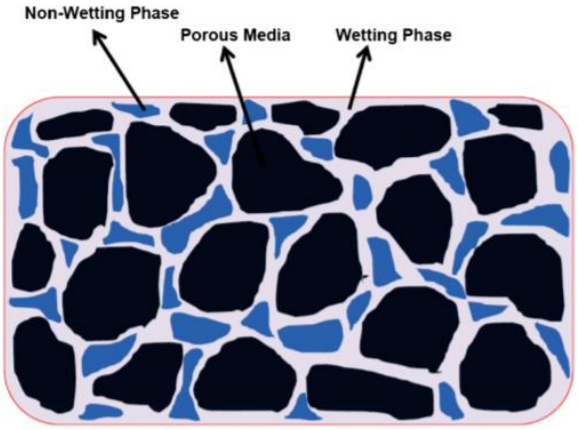

Figure 2. 1: Pore cross-section with general wetting and non-wetting phase distribution [13].

Other types of wettability are mixed wet and fractional wet. At mixed wet conditions, tiny pores in the rock act as water-wet and soaked water, while larger pores are oil-wet and oil contact with pore walls creates a continuous path through the rock length. The heterogeneous wetting of the pore surface can be characterized by fractional wetting. Besides, fractional wettability is also used for different reservoir parts/zones of different wettability characteristics. In this situation, some parts of the reservoir can be more water-wet than others.

2.1.3 Measurement of Wettability

Several methods have been invented for the measurement of wettability [14]. These methods can be divided into two groups: quantitive and qualitative. Among quantitive methods are contact angle, imbibition, forced displacement, and the United States Bureau of Mines (USBM) method. Other types of techniques are qualitative methods consisting of microscopic examination, imbibition rates, relative permeability curves, permeability/saturation relationships, capillary pressure curves, displacement capillary pressure, and reservoir logs [14]. Even with so many methods to infer actual wetting state, one approach is not enough to determine wettability conditions, and several techniques are often applied to characterize wettability conditions [15].

2.1.3.1 Quantitative Methods:

i. Contact-Angle Method

Contact angle forms when a drop of water is placed on a surface immersed in oil [14], and the rule is to measure the contact angle through the densest phase. This angle between the surface of liquid and solid can range from 0° to 180°. When the contact angle is less than 90°, the surface is preferentially water-wet. Accordingly, when it is greater than 90°, it is considered to be oil-wet. However, the angle can be equal to 90°, inferring the true wetting state as intermediate or neutral-wet [14].

In Figure 2.2 (a), the contact angle between liquid and solid is less than 90°, which makes this system water-wet, and hence water has a higher affinity towards the solid. Nevertheless, in (b), the droplet's contact area with solid minimized, which contributes the contact angle to be greater than 90° indicating oil-wetness. Finally, in (c), the system showing neutral wetness due to both fluids have an equal preference towards the solid surface.

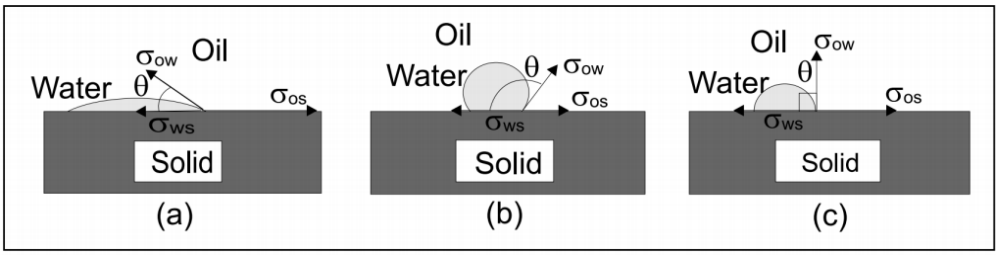

Figure 2. 2: Three surfaces with different wettability [16].

(a) water-wet ($\theta < 90^\circ$), (b) oil-wet ($\theta > 90^\circ$), and (c) neutral-wet ($\theta = 90^\circ$)

The contact angle is the best wettability measurement method when pure fluids and artificial cores are used [14]. At the same time, it can also be applied to estimate wettability when nanoparticles and surfactants are used. In addition, the technique is suitable for checking if crude oil can alter wettability and determine the effects of temperature, pressure, and brine chemistry on the wetting state. For contact-angle measurements, many methods have been applied: sessile drops or bubbles, vertical rod method, tensiometry method, cylinder method, and capillary rise method [14].

Generally, in the petroleum industry, the sessile drop and modified sessile drop methods are used [14]. The main difference between these methods is the number of polished mineral crystals. There is one in the sessile drop method, while in the modified sessile drop method, there are two. As shown in Figure 2.3, polished mineral crystals are mounted parallel to each other on adjustable posts in the modified sessile drop method.

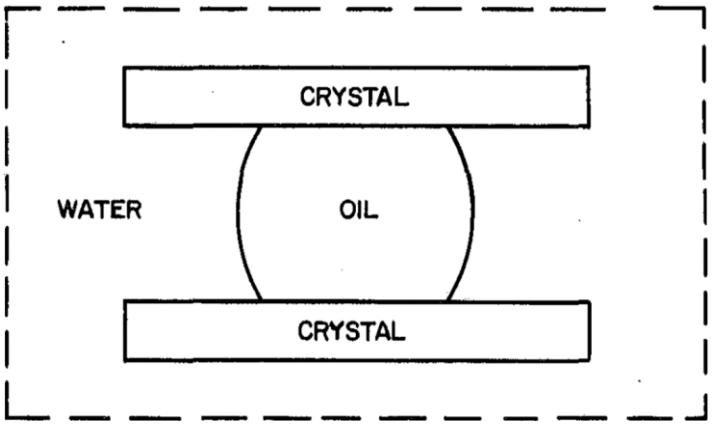

Figure 2. 3: Contact-angle measurement by modified sessile drop method [14].

Among all methods for determining wettability, the contact-angle is one of the simplest and cheapest ways for cleaned and smooth surfaces. Moreover, it is suitable even for non-porous mediums. Unfortunately, the wetting state quantified with this method may not represent the actual reservoir rocks because some essential factors like reservoir heterogeneity, surface

roughness, and pore geometry are not considered during the measurement process. It is proved that roughness and pore geometry significantly impact the state of wetting [17].

ii. Amott Method

The Amott method was developed for measuring the average wettability of a rock sample by combining forced displacement and imbibition [18]. Moreover, in the Amott method, both the rock samples and fluids from the reservoir can be used.

This method is based on the displacement of the non-wetting fluid in the sample by the spontaneously imbibed wetting fluid. Amott index is the ratio of spontaneous imbibition to forced imbibition. The Amott index is utilized to reduce the influence of factors such as relative permeability, viscosity, and initial saturation of the rock [18].

The Amott test can be summarized in four steps:

1. To imbibe water spontaneously, the core sample at irreducible water saturation is put in a water-filled tube (from S1 to S2 in Figure 2.4).

2. Oil saturation reaches irreducible oil saturation by the displacement of the remaining oil in the core (S2 to S4). The recovered oil (due to spontaneous imbibition and forced displacement) is noted.

3. The amount of water superseded because of spontaneous imbibition of oil is noted after the sample is submerged in oil for about 20 hours (S4 to S3).

4. The remaining water is displaced by forcing oil through the sample, which is placed in the flow cell (S3 to S1). A total amount of water displaced (both by spontaneous imbibition of oil and forced displacement) is noted.

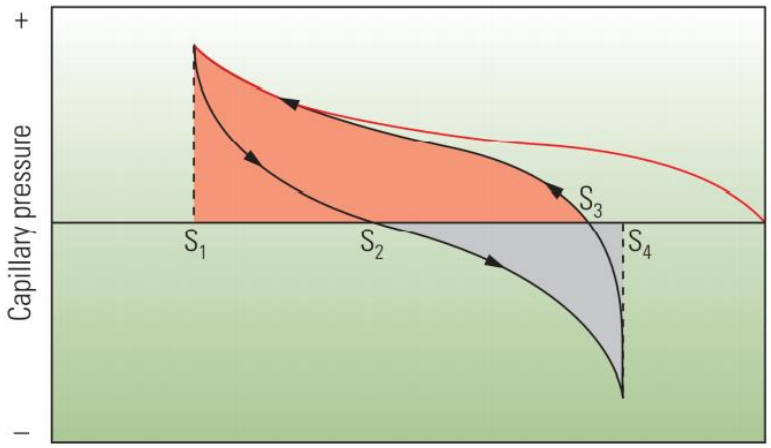

Figure 2. 4: Capillary pressure water saturation in Amott test [19].

Separate ratios of spontaneous imbibition to total saturation change for water, I_w, and oil, I_o, are termed the water and oil imbibition indices, respectively.

$$I_O = \frac{(S4-S3)}{(S4-S1)} \tag{2.1}$$

$$I_W = \frac{(S2-S1)}{(S4-S1)} \tag{2.2}$$

At the strong oil-wet conditions, I_O is close to 1, whereas I_W is close to 0. On the other hand, in a strongly water-wet core, I_W is close to 1 while I_O is close to 0.

The Amott-Harvey method is a modification of the Amott method and index for this method denoted by I_{AH}, which identifies the core sample's wettability [18]. The designed conversion is comprising of varying the way forced displacement is implemented. During this method, the displacement is carried out with Hassler Core Holder, a suitable method for utilizing external pressure. Before running the genuine test, there is an extra step in preparing the sample, replacing the core in the Core Holder: first in brine, next in crude oil to reach the irreducible water saturation. Afterward, the displacements by water and oil are calculated. The relative Amott-Harvey displacement index is the displacement by water ratio minus the displacement by oil ratio, as illustrated in Figure 2.5 [18].

$$I_{AH} = I_W - I_O \tag{2.3}$$

The index can range between +1 for the water-wet system and -1 for the oil-wet system. Moreover, when the index is close to 0, the system is considered as intermediate or neutral-wet.

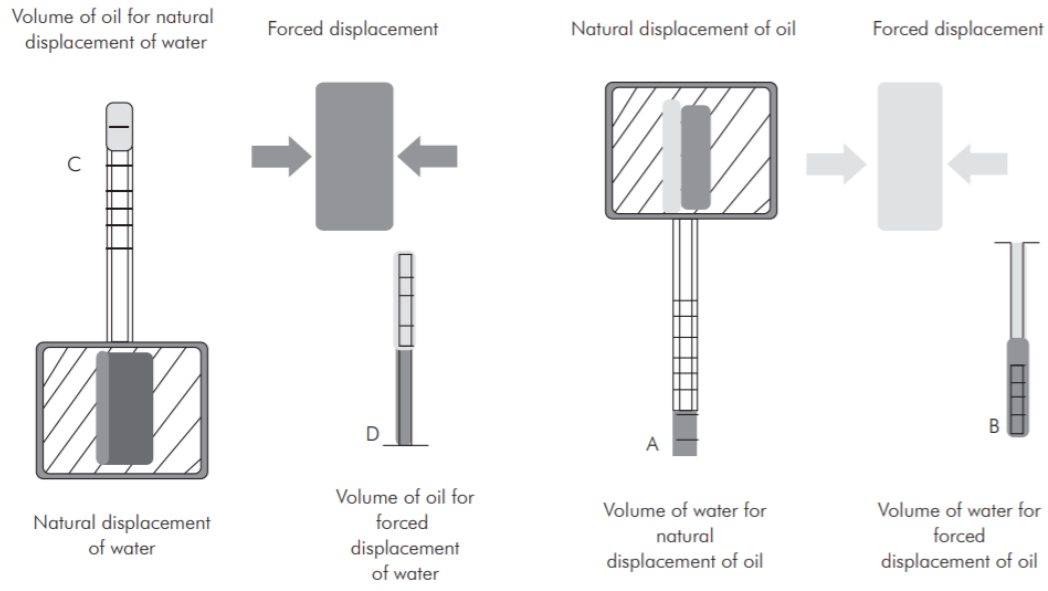

Figure 2. 5: Determining wettability by natural and forced displacement using the Amott-Harvey method [18].

iii. USBM method

The alternative method for measuring the wettability of the sample was developed by the USBM and Donaldson et al. [20]. By utilizing the USBM method, it is possible to perform four to eight tests in a few days and compare with other methods, i.e., it is relatively fast. Furthermore, one of the essential advantages of this method compared to the Amott test is the higher sensitivity near neutral wettabilities [18]. However, there is one disadvantage with the USBM; it is the limitation of a core sample size, which should be 3.5 cm in diameter and 5 cm in length in plug shape, due to the requirement for using a centrifuge. The method measurement is based on the work of one fluid to replace another fluid in a porous medium.

The required work is considered to be equal to the area under the capillary pressure work. From Figure 2.6a, it can be seen that in the water-wet state, the area under the capillary pressure curve of displacement by brine is smaller than the area under the capillary pressure curve for another displacement for water-wet reservoir condition. While, if the wetting state is oil-wet, the area under the displacement of the oil curve will be small due to the imbibition of most of the oil by the sample (Figure 2.6b).

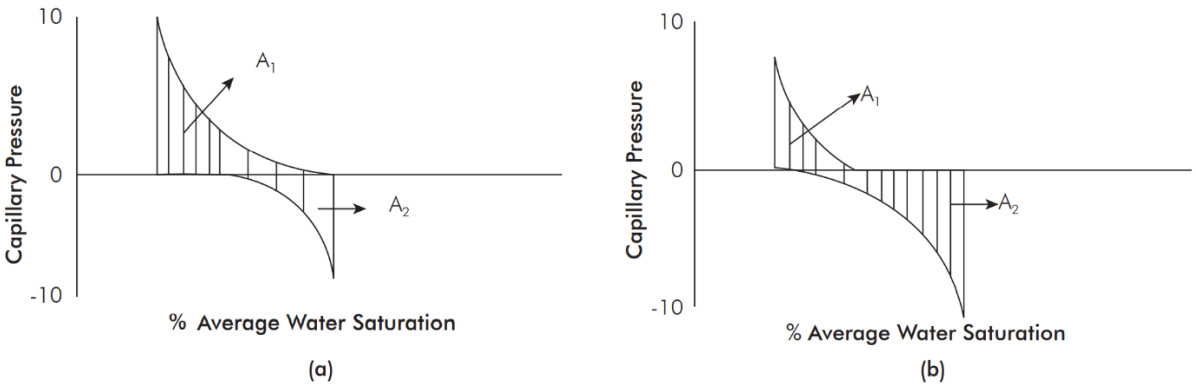

Figure 2. 6: USBM Method to determine wettability.

a) Water-wet, b) Oil-wet [14].

For calculation wettability by utilizing USBM, the equation below is used:

$$W = \log(\frac{A1}{A2}) \quad (2.4)$$

When W is around 1, the wettability is considered water-wet, about 0 neutral, and near to -1 is oil-wet.

2.1.3.2 Qualitative Methods

The primary purpose of qualitative methods is to characterize the wetting state of the rock without using this preference's quantitative limits. There are different methods of this type [18], e.g.:

- Visual method.
- Imbibition method.
- Relative Permeabilities method.
- Capillary Pressure method.
- Flotation method.

However, in this study, just the imbibition, relative permeabilities, and capillary pressure methods are discussed.

i. Imbibition method

Among qualitative methods, wettability characterized by the imbibition method is the most common due to giving quick and accurate information about the wetting state without demanding the use of sophisticated technology to run the test. The procedure is based on the flow rate of wetting fluid which replaces the non-wetting fluid with the simple action of capillary forces [18]. If the flow rate and the water volume are significant, the core is strongly water-wet; otherwise, it is weakly water-wet or oil-wet. This scenario can also be applied to the oil-wet core. [14].

ii. Relative permeabilities method

Relative permeability and wettability are interdependent parameters and based on this fact, some methods for measuring wettability are introduced [21]. Wettability affects the distribution of water and oil and their movement through pore spaces. Therefore, the effect of wettability on the flow behavior of reservoir fluid is reflected in relative permeability. However, these methods can only determine strong water-wet cores and strong oil-wet cores, i.e., not the minor changes in wettability. For example, alteration between the core that is heavily wet by water and moderately wet by water may not be noticed by these methods [21]. Figure 2.7 (a) shows that the crossing point of permeability curves is at more than 50% water saturation due to water being the wetting fluid. On the other hand, in Figure 2.7(b), the crossing is less than 50% water saturation, so the wettability of the sample is oil-wet.

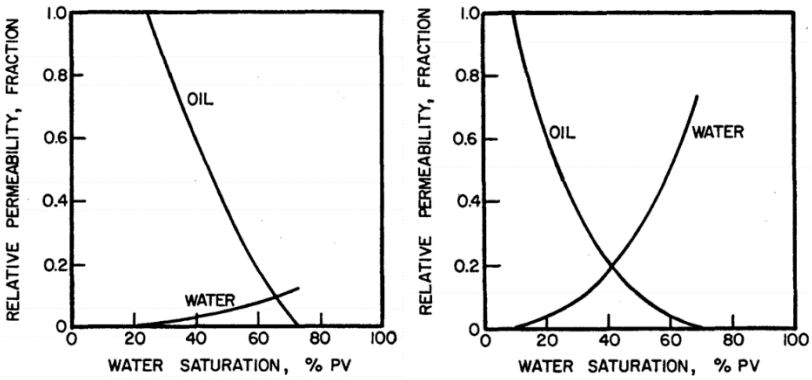

(a) Strongly water-wet (b) Strongly oil-wet

Figure 2. 7: Typical relative permeability curves [22].

iii. Capillary pressure method

Qualitative methods for measuring the wettability of porous medium can be created by utilizing several ways to determine capillary pressure. One of the most common methods is the Capillarimetric method [23], which recognized the priority of the fluid used to determine wettability. Figure 2.8 illustrates that this equipment binds two liquid phases: oil and water, through a capillary tube, with a capillary pressure using the interface of the phases.

The principal measured parameter in this method is adhesion tension in a capillary tube. This parameter can be determined by the distinction in the heights of the fluids in the equipment parts. This inequality between heights is happening due to the difference in densities and acceleration of water and oil gravity.

$$E_D = \sigma\cos\theta = 70.307\frac{r}{g}(\rho_o h_o - \rho_w h_w) \quad (2.5)$$

Where:

E_D = Displacement energy, psi

r = pipe radius, cm

g = Gravity, cm/sec

ρ_o = Oil density, gr/cm^3

ρ_w = Water density, gr/cm^3

h_o = Oil height, cm

h_w = Water height, cm

From the equation above, the energy displacement can be calculated. A positive result means that it is water-wet, while a negative result means oil-wet.

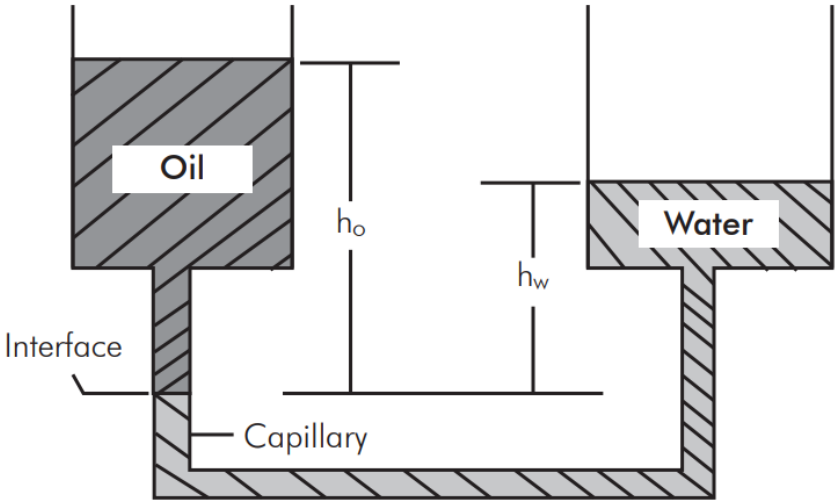

Figure 2. 8: Capillarimetric method [21].

2.1.4 The Influence of Wettability on Oil Recovery

The interplay of many interacting factors, mechanisms, properties, etc., at the pore levels and macroscopic scales can affect oil recovery efficiency [11]. For several decades, all these interacting forces have been among the main topics for scientific research in the oil industry [11].

The wettability of the reservoir rock is among the main factors that affect oil recovery efficiency [24]. While the rocks are hydrophilic, the oil is not the wetting fluid, and it is mainly found in large pores of the rock matrix. Therefore, under the influence of a pressure drop in the wellbore during the primary oil recovery methods, the oil has relatively high mobility and easily moves in its direction. However, when the reservoir rocks are hydrophobic, oil is located in tiny pores, so the extraction process becomes harder than hydrophilic rocks [24].

The relative permeability is a crucial parameter in the pore displacement of individual phases in the reservoir [25]. This parameter is a function of the history of saturation, pore geometry, distribution of fluids in the rock, and wettability. Hydrophilic rocks have a higher oil permeability than water, while if the rock is hydrophobic, it will be the opposite. Therefore, oil extraction from hydrophilic reservoir rocks is more significant due to the higher relative permeability of oil.

2.2 Factors Affecting the Wettability

Primarily factors affecting the reservoir wettability are the rock properties and the characteristics of the reservoir fluids [26]. Moreover, some aspects also have a role in the alteration of the wettability, such as temperature and pressure, location of fluid contacts, etc. Nevertheless, uncertainties in the relative importance of these various factors on reservoir wettability still exist [26]. Therefore, this section will discuss the following factors affecting reservoir wettability: oil and brine compositions and reservoir rock mineralogy.

2.2.1 Oil Composition

The crude oil composition affects reservoir wettability; however, it is hard to determine which components of the reservoir oil have an essential impact on wettability alteration [26]. On the other hand, it is widely agreed that the existence and amount of polar components, such as asphaltene and resin, affect the wetting state of the reservoir [26]. The polar oil components absorb onto the rock surface if there is no water layer between rock and oil. In the presence of water, the polar oil components and negatively charged mineral particles are connected by di- and three-valent cations that act as cation bridges, and direct adsorption is also possible [27]. Due to the variety of the internal structure of rocks, such as mineral surfaces and shape of pore space, it is hard to evaluate the underlying mechanisms by studying core samples [27]. Research about the effect of asphaltenes on the reservoir rock's wetting state shows that asphaltenes in crude oil alter wettability towards oil-wet. In the following, some investigations are discussed to find out the effect of oil composition on the wettability state in the reservoir:

- Rayes et al. [26] chose a Hungarian and a Libyan oil field to study their oil-water-rock system and understand how asphaltene affects the wetting state. After measuring the system's contact-angle in several tests, they determined that asphaltenes can substantially modify the wetting characteristics of rocks. The results indicated a significant alteration in the wetting angle from 40°-60° to 120°, which meant that the oil-wet state replaced the water-wet state.
- Liu and Buckley [28] studied wettability change by adsorption of asphaltenic components. As the test solid surface, a borosilicate glass microscope slide was utilized, and this surface was aged in four different asphaltenic crude oils. Measuring the solid surface's contact angle before and after aging in crude oil gave similar results to those of Rayes et al. [26]. The degree of contact angle changed from 50°-70° to 170°.

Moreover, the studies of the main mechanisms of COBR interactions indicated that if there is no water layer between the solid and oil, the polar interactions between asphaltenes and solid are dominant. Crude oil can act as a solvent for asphaltenes and plays an essential role in the oil/rock system. When the oil acts as a poor solvent for asphaltenes, the system's wetting state becomes more oil-wet [27].

Polar components in the oil can still affect the wettability in the presence of water film between oil and solid if the water contains calcium (Ca^{2+}) cations. The particular reason for this circumstance is the act of Ca^{2+} as a cation bridge that connects negatively charged rock and polar components of oil and leads the wetting state to be oil-wet.

2.2.2 Brine composition

Crude oil chemistry or composition influences the wettability condition of oil/water/rock interactions. However, some studies about wettability alteration showed that brine chemistry or design also affects the system's wettability:

- Vijapurapu and Rao's [29] study is based on the effects of brine dilution on the wettability of the oil/water/rock system where the solid surface was dolomite. They found that diluting the reservoir brine with deionized water can change the wetting state from oil-wet to intermediate wet. Moreover, the experiments done by Al-Aulaqi et al. [30] demonstrated how the wettability state of the oil/water/rock system was altered when the temperature and brine salinity were adjusted. The results indicate that reducing the brine salinity with monovalent cations changes the wettability of the system to more water-wet conditions.
- The displacement experiments on different oil-brine systems and Berea sandstone were done by Tang and Morrow [31], showing that temperature increase and salinity reduction altered the wetting state to more water-wet. The influence of low salinity water on oil production and interactions between cations in brines of low and high salinity were studied by Fjelde et al. [32] for a sandstone with high clay content. First of all, the core sample was prepared with FW afterward, at initial saturation water, it was aged in crude oil. Then, prepared core plugs were either flooded by FW, seawater, low salinity water in sequence, or low salinity water directly from saturation water. The results showed that the high salinity FW kept the rock's wettability in water-wet condition; however, low salinity water changed it to less water-wet.

The wettability of sandstone and dolomite tend to be water-wet in the presence of the low salinity water compared to brines of higher salinity [32]. Nevertheless, a different result was found for reservoir rock with high clay content by Fjelde et al. [32]. Where the low salinity water changed wettability towards oil-wet state rather than water-wet. In the previous study, which was mentioned in Chapter 2.2.1 [27], it was found that a higher concentration of Ca^{2+} can contribute to more water-wet conditions if the crude oil is rich with polar components. In other words, high salinity water is more sensitive to a high concentration of polar components in crude oil, so the interaction between oil/cation/rock has an essential impact on the wettability state of the rock.

2.2.3 Reservoir-Rock Mineralogy

Another essential factor for the wettability of the reservoir is rock mineralogy [33]. The reservoir rock characteristics are determined by its porous, permeable, and lithological structure, and these rocks are also known as sedimentary rocks. Moreover, sedimentary rocks may be made of sandstones, carbonate mud, or dolomite. Various studies were examined to determine how rock compositions of sandstone reservoirs and carbonate reservoirs affect wettability:

- Both studies, which were done by Treiber et al. [34] and Chilingar and Yen [35], indicated that the wettability state in carbonated reservoirs is typically more oil-wet than sandstone reservoirs. Nevertheless, there are some exceptions, such as chalk on the Norwegian Continental Shelf (NCS).
- Erzuah et al. [36] utilized Surface Complexation Modeling (SCM) with the help of a geochemical model (PHREEQ-C) for studying the wettability of the minerals (quartz, kaolinite, and calcite) [37]. Along with this model, similar flotation tests were examined for confirmation of estimated wettability state of the minerals. The oil wetness was found to decrease in order calcite > kaolinite > quartz. The primary wetting mechanism for calcite was direct adsorption of carboxylate on the positively charged calcite surfaces, while for quartz and kaolinite it was cation bridging.

2.3 CO_2 Properties

2.3.1 Physical Properties

At normal conditions (T = 20 °C and P = 1 atm), CO_2 is gaseous and its density is approximately 1.98 kg/m^3 [38]. CO_2 is a colorless and odorless gas at standard temperature and pressure; however, CO_2 also can exist as a liquid, solid, or supercritical fluid. The properties of CO_2, such as density and viscosity, vary significantly between these phases. The phase diagram in Figure 2.9 shows the alteration of the physical state of CO_2 with pressure and temperature [38].

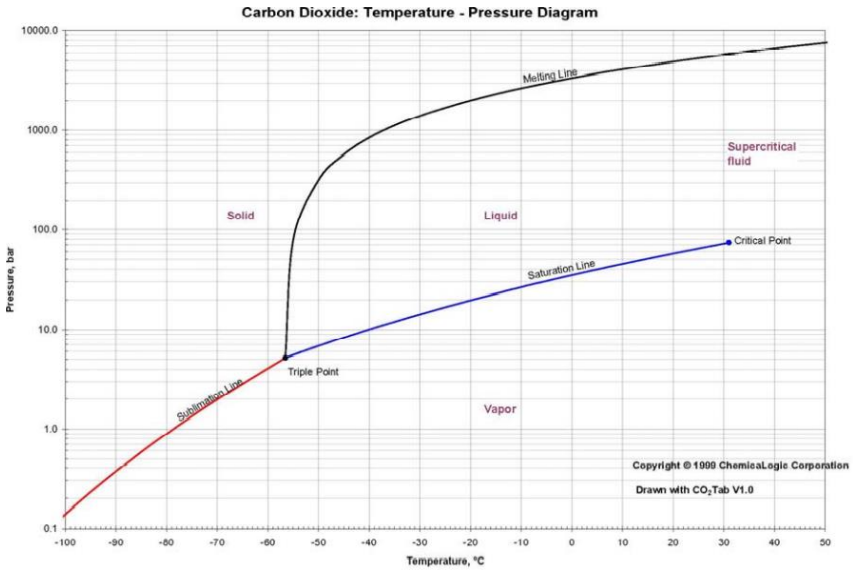

Figure 2. 9: Phase diagram of CO_2 [38].

At low-temperature and high-pressure conditions, the phase change from gas to liquid can be noticed, leading to a density increase [39]. The supercritical phase can be reached at temperatures and pressures higher than approximately 31.1 °C and 73.8 bars, respectively. There are no separate liquid and gas phases in the supercritical region. Moreover, pressure increase contributes to a steady rise in density [38]. The viscosity of CO_2 in the supercritical state is like that of gas; however, density is similar to that of a liquid phase [2].

CO_2 can usually be found in depth between 800 m and 3000 m in reservoirs, and the phase state is typically liquid or supercritical liquid due to the pressure and temperature conditions associated with these storage depths [40]. Temperature, pressure, and salinity are the main factors determining CO_2 and the physical properties of water, such as density and viscosity [40]. Water can be considered incompressible due to the narrow density range even in the reservoir condition, while CO_2 is compressible, and its density range can vary between 266 and 800

kg/m^3. Moreover, at high-pressure conditions, CO_2 density can even approach or exceed the water density [2].

2.3.2 Chemical Properties

CO_2 is the atmosphere's component; along with it, CO_2 also dissolves in the water of lakes and oceans [38]. The solubility of CO_2 is approximately 90 cm^3 per 100 ml of water at a temperature of 25°C, and there are various forms of CO_2 in an aqueous solution. The first dissolution step of the gaseous CO_2 [38]:

$$CO_2(g) \leftrightarrow CO_2\,(aq) \tag{1}$$

During the dissolving process in the aqueous solution, CO_2 forms carbonic acid (H_2CO_3) from the reaction with water, which immediately separates into bicarbonate (HCO_3^-) and carbonate (CO_3^{-2}) ions [41]. These processes can be seen in the following equations:

$$CO_2(aq) + H_2O \leftrightarrow H_2CO_3(aq) \tag{2}$$

$$H_2CO_3(aq) \leftrightarrow HCO_3^-(aq) + H^+ \tag{3}$$

$$HCO_3^- \leftrightarrow CO_3^{2-}(aq) + H^+ \tag{4}$$

The pH of the water drops because of the release of the proton, H^+, which was shown above by equations (3) and (4). Furthermore, the pH number can drop to three and even lower [39].

2.4 Fundamentals of Enhanced Oil Recovery Methods

Commonly, oil recovery methods are divided into three stages: primary, secondary, and tertiary [42]. Primary recovery is the first stage of hydrocarbon production, and during this stage, hydrocarbons are displaced from the reservoir into the wellbore and up to the surface by natural reservoir energy. In the beginning, the remarkably high natural differential pressure between reservoir and bottom hole contributes to hydrocarbon production. Nevertheless, due to the production, the reservoir pressure decreases, leading to a decline in differential pressure. An artificial lift system such as an electrical submersible pump or rod pump can be applied to increase hydrocarbon production in this scenario. Two main factors indicate when the primary recovery reaches its limit, and these factors are a high proportion of water or gas in production steam and external differential pressure, which leads to non-economic production.

Generally, only 10% of the initial oil in place can be produced during the primary recovery stage [43]. After primary recovery reaches its limit, usually secondary recovery stage is

implemented. The most common secondary recovery methods are water flooding and gas injection, which help control reservoir pressure and displace hydrocarbons for production. This stage also reaches its limit when the production is economically unreliable, and the injected fluid is indicated in high amounts in the production stream. However, for this stage, the recovery factor is higher compared to the primary recovery and can range between 15% and 40% [44]. However, exception in these recovery steps is NCS, where water is injected from day one, e.g., directly to secondary recovery.

When the secondary recovery process becomes unprofitable, tertiary recovery methods are applied to improve the oil recovery of the reservoir. In tertiary operations for the oil displacement, the miscible gases, chemicals, and thermal energy are utilized [42]. EOR is a synonym term for tertiary recovery. Moreover, as EOR methods can be used in any reservoir development stage, the term tertiary recovery is not used so often nowadays [45].

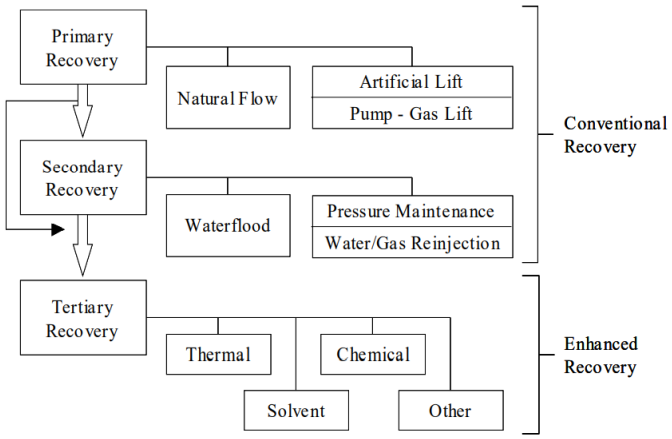

Figure 2. 10: Oil recovery classifications [46].

2.4.1 Enhanced Oil Recovery

EOR is an injection of materials that do not commonly exist in a reservoir for developing oil recovery [46]. As explained previously, when rock behaves more oil-wet, the recovery rate becomes lower. The majority of the accomplished EOR methods' goal is to increase oil recovery by changing the wettability toward more water-wet [7].

The level of the water-wet state that can be reached by the EOR method excessively relies on how it alters COBR properties. Moreover, for each petroleum reservoir, crude oil interaction processes with rock and brine are different. These procedures mainly depend on rock mineralogy, crude oil and brine compositions, and other reservoir properties [7]. A general schematic of the EOR process is shown in Figure 2.11.

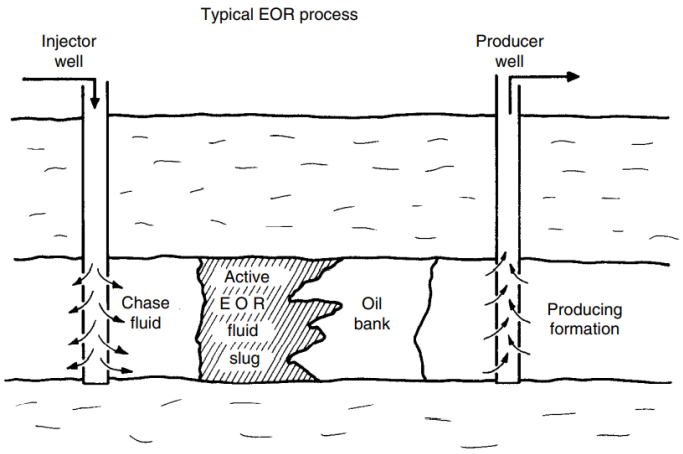

Figure 2. 11: General schematic of enhanced oil recovery [47].

Very often, EOR methods are classified as given in Figure 2.12.

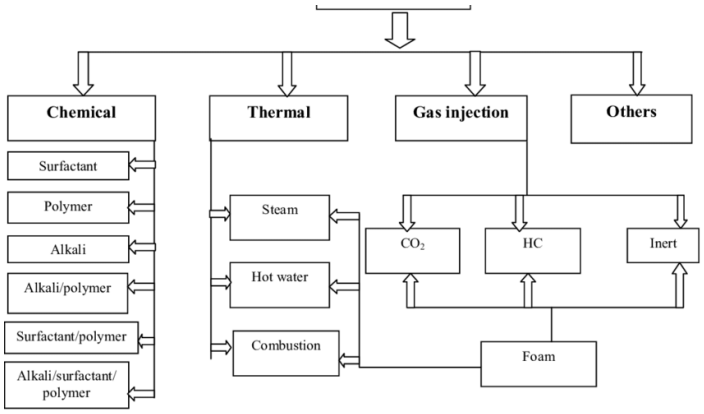

Figure 2. 12: Classification of EOR methods [48].

One of the oldest methods used by engineers to increase oil recovery is a gas injection [47], [49]. And the most common gas injection method is CO_2 flooding due to its high productivity and cost-effectiveness. More detailed information about CO_2 effectiveness in recovery is given in the next chapter.

2.4.2 Carbon Dioxide Flooding

The injection of CO_2 into an oil reservoir to increase the oil recovery factor is known as a CO_2 flooding process (CO_2-EOR) [48]. There are several reasons why CO_2 flooding is effective for oil recovery, such as reducing crude oil viscosity, swelling of crude oil, miscibility effects, an increase of injectivity, and internal solution gas drive [50]. During CO_2 flooding, CO_2 swells the net volume of oil and decreases its viscosity even before vaporizing gas drive mechanism achieves miscibility. It is because of the high solubility of CO_2 in crude oil at reservoir pressures [47].

CO_2 flooding is more effective in reservoirs deeper than 2000 ft, where it will reach its supercritical state and be miscible with crude oil, with oil gravity higher than 22-25° [51]. As a result of the written above, it can be concluded that the primary mechanism in CO_2 flooding is a generation of miscibility between the oil and the CO_2, and it can exist in crude oil and CO_2 system if the pressure is high enough. This pressure level is also known as Minimum Miscibility Pressure (MMP) and has been a target of several laboratory investigations [47]. Correlation between the API gravity and the required MMP shows that temperature growth tends to increase the MMP. It was demonstrated by the 1976 National Petroleum Council (NPC) report [52].

Furthermore, some studies showed that the reservoir pressure should be high enough to reach minimum density in the CO_2 phase [53], [54]. CO_2 acts as a suitable solvent for the oil at the minimum density state, and MMP can be generated to provide the efficient displacement of the crude oil. Therefore, higher pressures are needed at more elevated temperatures to increase the CO_2 density to the same value as observed for the MMP at the lower temperature. Alteration of MMP with oil composition and the temperature is given in Figure 2.13.

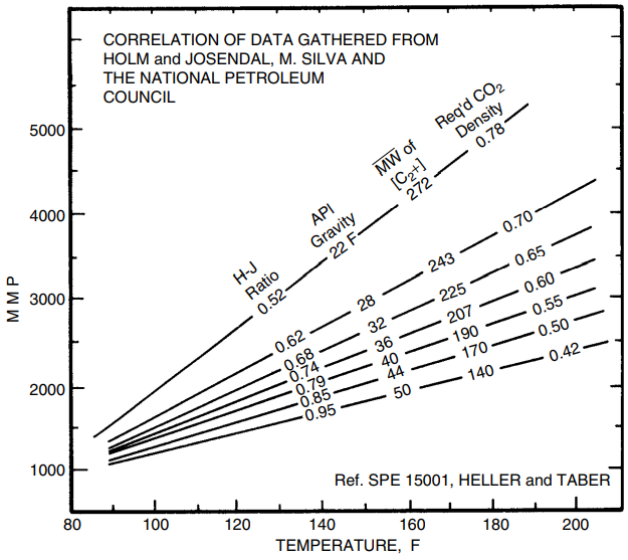

Figure 2. 13: Correlations for CO2 minimum miscibility pressure [55].

Before starting CO_2 flooding, the first action is to restore reservoir pressure to one suitable for production if the reservoir is very depleted [51]. It can be achieved by injecting water with the production well shutoff. After pressure development, CO_2 can be injected into the same injection wells used to restore pressure. Afterward, CO_2 is required to come into contact with the oil, and this process creates a miscible zone that can be transferred to the production well. More water can be injected during CO_2 flooding, where water sweeps oil to the production zone [51]. The CO_2 miscible process is illustrated in Figure 2.14.

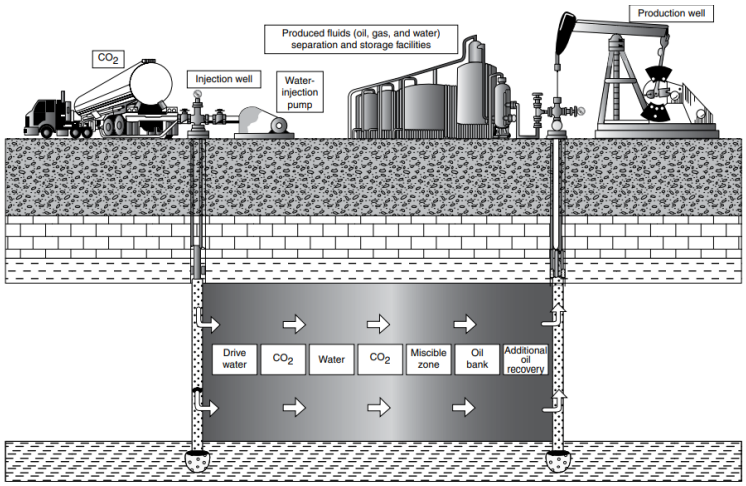

Figure 2. 14: CO_2 miscible process [42].

Mobility control of the injected CO_2 is poor due to low viscosity. Moreover, CO_2 tends to finger and breakthrough to the producer well, leaving large reservoir areas unswept. This issue can be solved by injecting alternating slugs of gas and water, known as a Water-Alternating-Gas process (WAG). Utilizing the WAG process can decrease viscous instabilities, which contributes to oil recovery increase. During the gas injection, gas can still tongue upwards in the formation away from the wells, while in the water cycle, water can move downward [51], [56]. The vertical permeability and density difference between the gas and reservoir fluid leads to the segregation of fluids. This process is visualized in the plot given in Figure 2.15. One of the essential factors during the WAG process is adjusting the correct volume of injected water and gas. Otherwise, too much water or too much gas can provide weak vertical sweep efficiency [56].

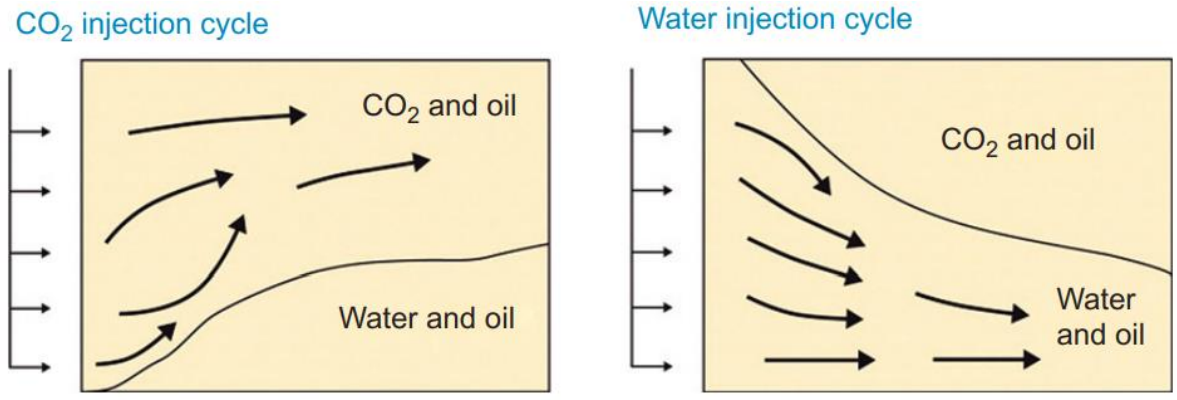

Figure 2. 15: During WAG, gas can move upward owing to its low density, while injected water can move downwards [57].

Earlier, the majority of the CO_2 utilized for EOR has been derived from naturally occurring reservoirs. However, modern technologies can produce CO_2 from industrial applications such as fertilizer, natural gas processing, ethanol, and hydrogen plants [51]. Dakota Gasification

Company's plant in Beulah, North Dakota, can be shown as an example of where CO_2 is produced and transferred by a new 204 mi pipeline to the Weyburn oil field Saskatchewan, Canada. In this oil field, for extending the field's productive life, CO_2 is injected, and this process can add another 25 years and around 130 million barrels of oil to the reservoir's production process.

2.5 Previous Work on Wettability Alteration

Wettability alteration is a practical approach to EOR [27]. There are several main factors affecting wettability alteration: rock surface mineralogy, oil composition, brine chemistry, and system temperature, pressure and saturation history [27]. Previous works on wettability alteration have attempted to answer how these factors affect the wetting state of the individual minerals and reservoir rocks by simulations and laboratory work. Each has its pros and cons, so its association is vital for understanding the wettability alteration process.

2.5.1 Experimental Work

Determining the wettability alteration during the water and CO_2 flooding is a complex process in the real reservoir [6]. It is essential to perform experiments on a small scale in the laboratory, representing the processes occurring on a large scale in the reservoir. Previous experimental work on wettability alteration mentioned in this study includes core experiments and flotation tests. Researchers have demonstrated experimentally that the wetting state of the reservoir can be changed due to brine injection. Moreover, temperature and pressure effects on the wettability preferences of the minerals were also discussed.

2.5.1.1 Core Experiments

Core flooding experiments demonstrated that the oil recovery factor is maximum in neutral or slightly oil-wet cores [58], [59]. To investigate the effect of the wetting state on oil recovery, Al-Mutairi et al. [6] worked on wettability alteration during CO_2 immiscible flooding under low pressures in a watered-out reservoir condition. The study included experiments to measure the oil/brine contact angle on a core piece taken from a carbonate core in the presence of CO_2. The contact angle was determined at various times until equilibrium was gained. A simple model which predicts wettability alteration with time was developed [6].

Al-Mutairi et al. [6] planned to start with an oil-wet porous medium fully saturated with water at residual oil saturation and inject CO_2 gas into the system. The wetting state was expected to be altered from oil-wet to intermediate-wet as CO_2 was exposed through the oil and water to

the rock surface. The difference in concentrations of CO_2 molecules has an essential role in controlling the diffusion. The diffusion rate would diminish exponentially with time as such difference decreases [60]. The change in the contact angle was found to be directly linked to the concentration of CO_2 at the oil/rock surface. As the value decreased exponentially with time, the contact angle also exponentially decreased exposure time (Figure 2.16).

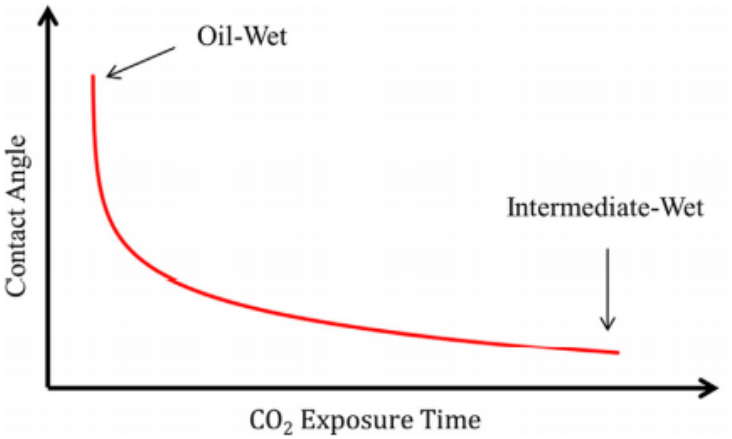

Figure 2. 16: Contact angle variation with CO2 exposure time [6].

The connection between wetting state and CO_2 exposure time can be given as follows based on the above concept:

$$\theta = ae^{-bt} + c \tag{2.6}$$

where:

θ = contact angle

t = CO_2 exposure time

a, b, and c = constants related to rock and fluid compositions as well as aging history and process parameters

Analysis of Eq (2.6) demonstrated that c is the ultimate contact angle (θ_{min}) achieved at infinite exposure time (i.e., $t \rightarrow \infty$). The difference between the initial contact angle (θ_i) and θ_{min} equals constant a. Constant b is relevant to the time when the contact angle is almost equal to θ_{min}. Such time can be defined as stabilization time (t_{sb}), and b can be given as $b = \varepsilon/t_{sb,}$ where ε is a constant.

Utilizing all the above parameters, Eq (2.6) can then be rewritten in dimensionless form as

$$\frac{\theta - \theta min}{\theta min} = \frac{\theta i - \theta min}{\theta min} e^{-\varepsilon/t_{sb}} \tag{2.7}$$

Defining dimensionless contact angle as $\theta_D = (\theta - \theta_{min})/ \theta_{min}$ and dimensionless time as $t_D = t/t_{sb}$, Eq (2.7) can be given:

$$\theta_D = \theta_{Di} e^{-\varepsilon/t_D} \tag{2.8}$$

where

$$\theta_{Di} = \frac{\theta i - \theta min}{\theta min} \tag{2.9}$$

Al-Mutairi et al. [6] utilized eight components in their experimental setup, as illustrated in Figure 2.17. For controlling CO_2 injection, the CO_2 cylinder was linked to a visual cell through a regulator. Moreover, the temperature and pressure of the visual cell were controlled throughout the experiment.

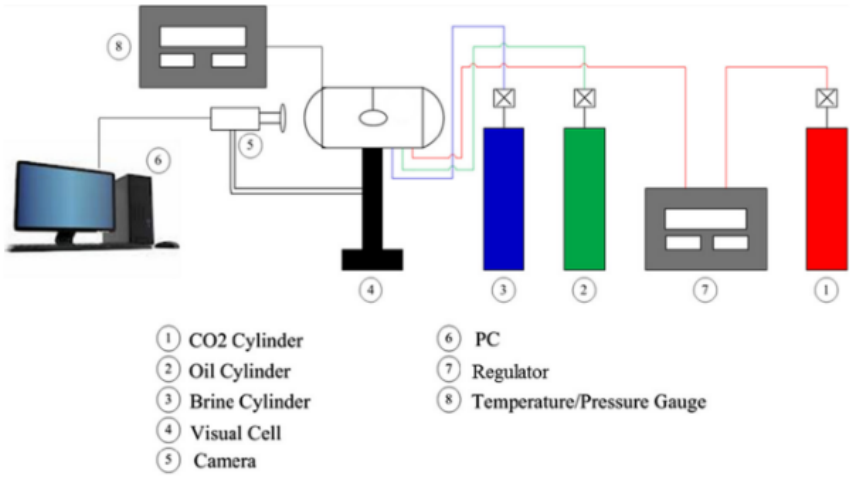

Figure 2. 17: Diagram of the experimental set-up [6].

The experiment was performed with two different brine CO_2 concentrations (0.0004 mol% for Run # 1 and 0.0008 mol% for Run # 2). Measured contact angles for these two cases were given in Figure 2.18. The contact angle measurement method was explained in Chapter 2.1.3. The results showed that CWI into carbonate rock causes alteration of the rock wettability from an oil-wet to an intermediate-wet state, and increasing CO_2 concentration in the brine leads to more alteration of the wetting state. Finally, after a short period, the COBR contact angle gained a new stable value.

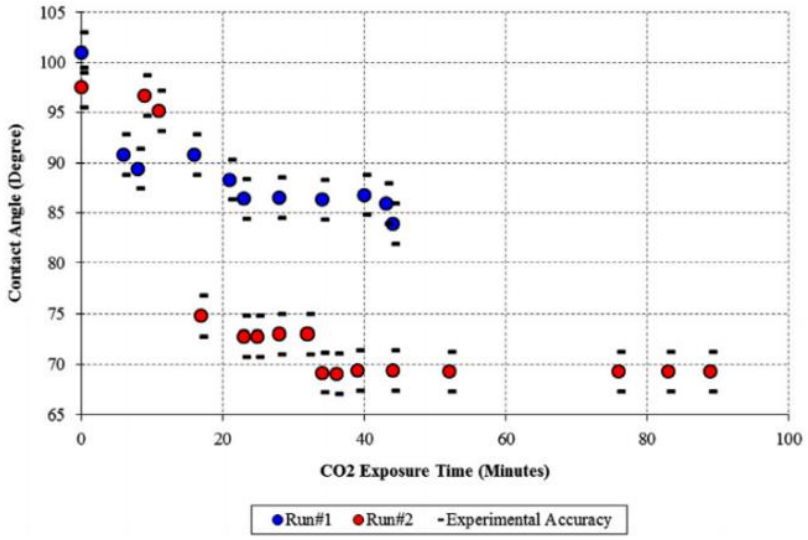

Figure 2. 18: Plot showing raw experimental data for Run # 1 and Run # 2 [6].

Another core experiment for visualization wettability alteration was done by Fjelde et al. [61]. The primary purpose of their study was to determine the wettability preference of the reservoir chalk rock after water flooding with FW, after spontaneous imbibition and water flooding by seawater, and after the first cycle of water alternating CO_2 flooding (CO_2-WAG). In the experiments, core plugs from a fractured chalk reservoir in the North Sea were utilized, and easily accessible sulfate was removed from the core plugs. Afterward, the wettability preferences of the chalk rock were determined by using stock tank oil (STO). The wettability conditions were characterized by the spontaneous imbibition of water and the water-wet area obtained by the sulfate wettability test.

First, the reservoir chalk plug was flooded by FW, and it appeared to be close to mixed-wet or preferential oil-wet. However, after spontaneous imbibition and viscous flooding with seawater, the wettability state of the core plugs became more water-wet than for the core plugs water flooded by the FW. Moreover, after applying CO_2 flooding on the same core plug, most of the oil was produced, and the wettability was altered toward more water-wet. Therefore, in the CO_2-WAG flooding experiments, the water-wet area of the core plug was also increased.

Zhang et al. [62] performed experiments using the captive bubble method to characterize the wettability of sandstone rocks and their mineral components before and after CO_2 injection. Berea and Obernkirchener sandstones were used as sample rocks in these experiments, and their mineral components were determined by applying X-ray Powder Diffraction and X-Ray Fluorescence Analysis. From the analysis, Zhang et al. [62] concluded that sandstones consisted of five dominant minerals: quartz, kaolinite, chlorite, microcline, and muscovite. The

wettability preferences were estimated using Scanning Electron Microscopy and Energy Dispersive X-ray Spectroscopy analyses. From the results, it was observed that the wetting state of the sandstones was strong water-wet. Furthermore, before CO_2 injection, quartz was strong water-wet, while kaolinite, chlorite, and muscovite were weak water-wet. After applying CO_2, the wettability preferences of the minerals altered toward more water-wet.

To better understand the temperature and pressure effect on the wetting state of the minerals and reservoir rocks, Zhang et al. [63] performed a core experiment using the captive droplet method. The experiment was performed in wettability measurement apparatus DSA100HP (Figure 2.19) to estimate the wettability preferences of seven minerals and two reservoir rocks at different temperatures and pressures. During the experiment, the temperature ranged from 35°C to 110°C, and the pressure ranged from 10 to 70 MPa. On the basis of the experimental results, increasing pressure from 10 to 70 MPa had no noticeable effect on the wetting state of the mineral, nevertheless of mineral types, in the COBR system. In contrast, the temperature effect on wettability depended on the wettability preferences of the mineral. For the water-wet mineral influence of the temperate was significant. Increasing temperature altered the wettability of the mineral toward more water-wet. However, for oil-wet and neutral-wet samples, the temperature impact on the wettability alteration was relatively weak.

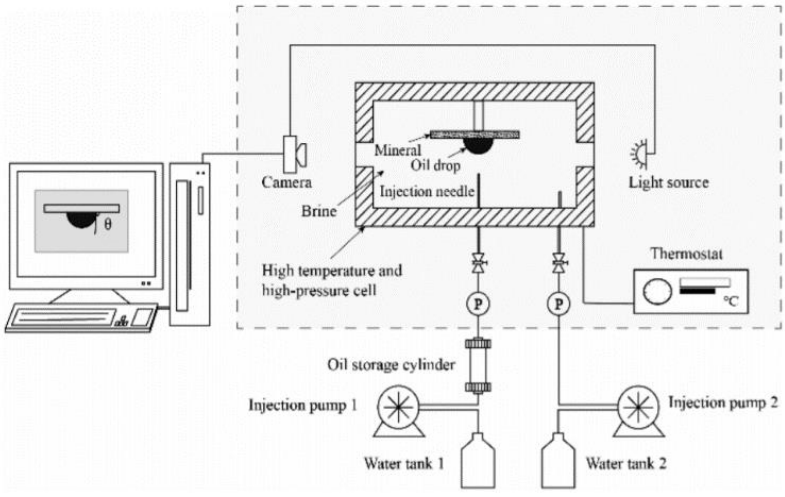

Figure 2. 19: Schematic diagram of the wettability measurement apparatus [63].

2.5.1.2 Flotation Test

Erzuah et al. [64] investigated the wettability preferences of the individual minerals, reservoir rocks, and mineral mixtures by using the flotation test and SCM. Nevertheless, in this chapter, only the flotation test results were presented. Flotation tests were performed for five dominant minerals in two sandstone reservoir rocks. Minerals existing in these reservoir rocks were:

quartz, albite, illite, montmorillonite and calcite. Besides minerals, two sandstone reservoirs and four PSR/mineral mixtures were also involved in these experiments. Mineral mixtures were designed to evaluate the impact of increasing surface area and calcite content; more detailed information was given in Chapter 3.

The experiment procedure started by selecting reservoir rock, crush it and sieve it through the mesh. Then, the sieved reservoir rock was taken and aged in the desired brine at the designated reservoir temperature (80°C) for two days (Section I of Figure 2.20). Afterward, the brine phase was split and kept for later use; meanwhile, the wet rock was aged with STO at the same temperature, intermittent stirring (Section II of Figure 2.20). The second part of the experiment imitated the rock fluid interactions in the reservoir during the accumulation of crude oil. Moreover, at the end of the second process, the separated brine was added to the aged rock to represent COBR interactions in the reservoir (Section III of Figure 2.20). The wetting state was determined based on the concentration of the rock/mineral sample in each fluid phase. Since it was challenging to separate the oil-phase from the oil-wet particles, unlike water-wet particles, the oil was discarded while the brine phase was filtered (Section IV of Figure 2.20). The next step was drying the filter cake until a constant weight was achieved. The difference between the initial weight of the chosen rock/mineral sample and the dried water-wet rock was used to calculate the concentration of the oil-wet particles. Furthermore, similar flotation experiments were carried out for mineral and mineral mixtures to estimate their wettability preferences. More detailed explanation of the flotation tests can be found in other literature [65]–[67].

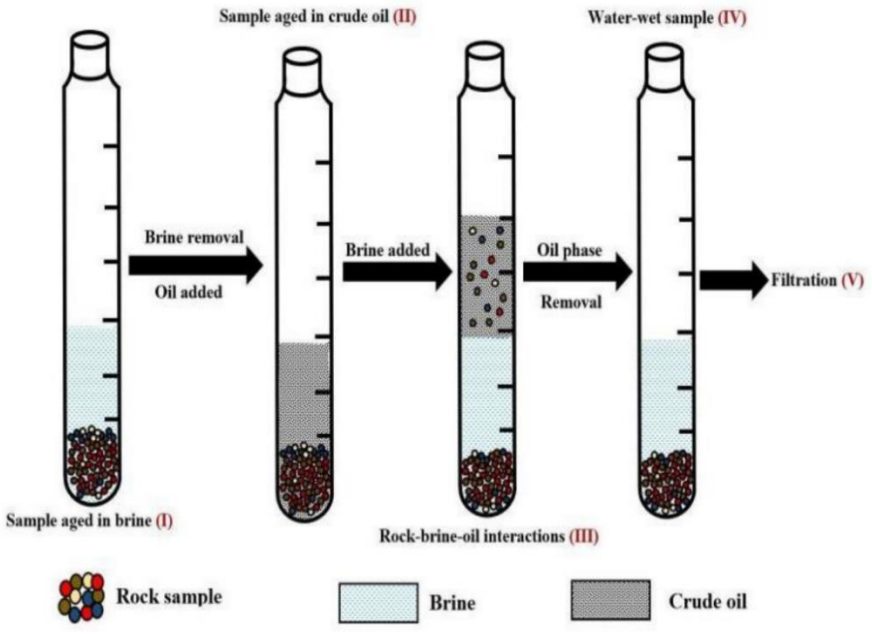

Figure 2. 20: Flow chart of the flotation experiment [64].

Results from flotation tests for individual minerals and sandstone reservoir rock/mineral mixtures were given in Figure 2.21 and Figure 2.22, respectively [64]. From Figure 2.21, it can be observed that the quartz was strongly water-wet, while calcite acted as strongly oil-wet. The wettability preference of the montmorillonite was more oil-wet than illite and albite. In other words, increasing order of the mineral hydrophobicity was given as quartz < albite < illite < montmorillonite < calcite.

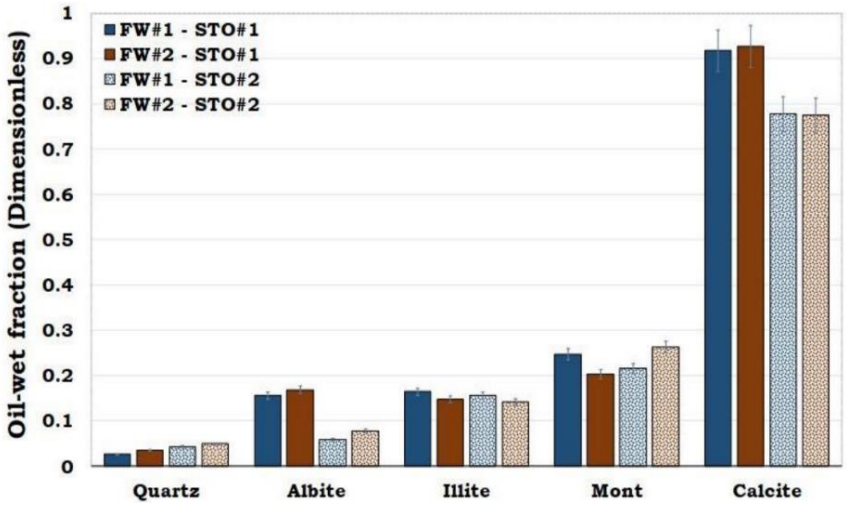

Figure 2. 21: Flotation tests results of the minerals [64].

From Figure 2.22, it can be observed that SRR#1 and SRR#2 were strongly water-wet, while PSR#4 acted as strongly oil-wet due to high calcite content. The wettability preferences of the other mineral mixtures were more hydrophobic than sandstone reservoir rocks (SRR#1 and SRR#2) and less hydrophobic than PSR#4.

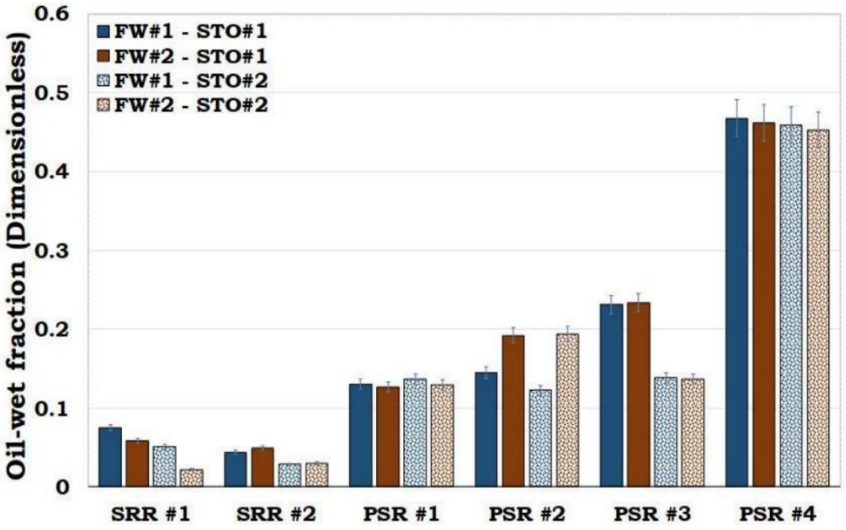

Figure 2. 22: Flotation test results of the sandstone reservoir rocks and mineral mixtures [64].

2.5.2 Simulations

There were some modeling studies on the determination wettability preferences of reservoir rocks and their dominant minerals. One of these simulation work principles is based on SCM. The SCM can be defined as a chemical model that uses an equilibrium approach to give a molecular description of adsorption phenomena [68].

The SCM is an economically attractive technique for characterizing the wetting state of minerals under reservoir conditions. Brines' ionic composition and the minerals' properties were utilized as input to the model. Besides, the polar oil components in the crude oil were transformed into their equivalent base and organic acid concentrations to be used as inputs to the model. The electric-double-layer model that was utilized in the SCM was the diffuse-layer model.

One of the essential features of the SCM is the possibility of studying electrostatic pair linkages existing between mineral/brine and oil/brine interfaces for a given reservoir condition. The fundamental reasons for the various SCMs are the location and surface configuration of the adsorbed ion at the rock/brine interface. The SCM can be termed a two-pK model that includes constant capacitance, diffuse layer, and triple-layer if the reactive surface functional group can experience protonation and deprotonation [68].

The previous work on SCM presented in this chapter is the second part of the Erzuah et al. [64] work where the prediction of the flotation tests via SCM was given. In their investigation, the attractive electrostatic interaction between the mineral-brine and oil-brine interfaces was studied using SCM to understand better the wetting state of the individual minerals, SRR, and PSR. Figure 2.23 and Figure 2.24 showed that the SCM could capture the trend of the flotation test results (Figure 2.21 and Figure 2.22). The results from SCM were defined by Total Bond Product (TBP), which is the sum of attractive electrostatic forces between the oil-brine and the rock-brine interfaces. More detailed information about the method is given in Chapter 3.

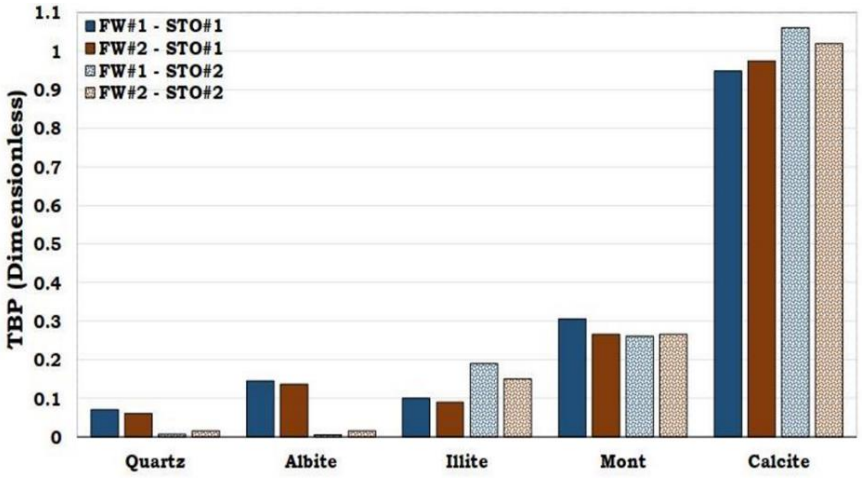

Figure 2. 23: Prediction of the oil adhesion tendencies of the individual minerals during the flotation test via SCM [64].

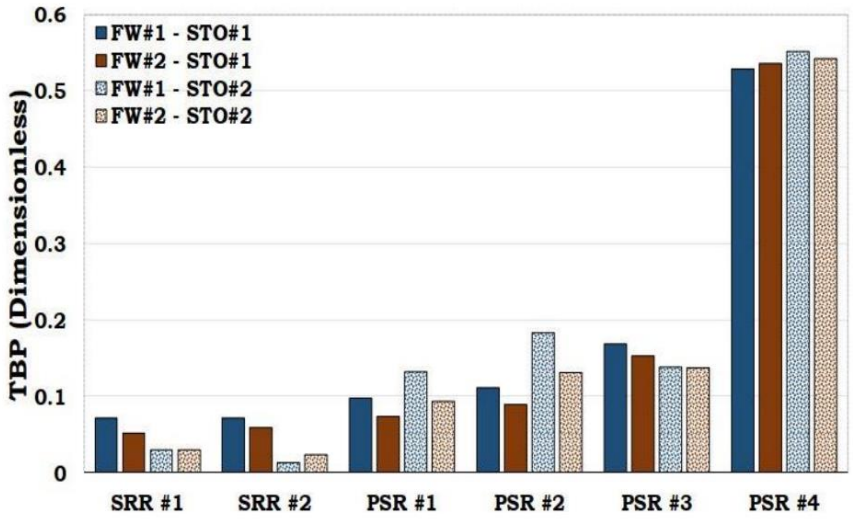

Figure 2. 24: Prediction of the oil adhesion tendencies of the reservoir rocks and mineral mixtures during the flotation test via SCM [64].

3 Simulation Method

In this section, input parameters of the simulation method are presented, such as individual minerals, mineralogical composition of the reservoir rocks and mineral mixtures. Furthermore, the properties of STO and brine types can be observed from the given tables in the present chapter. Moreover, the SCM method is also defined to understand the working principle of this method.

3.1 Minerals and Reservoir Rocks

The wettability of minerals and reservoir rocks at given conditions was estimated by using SCM. The simulation was performed for five dominant minerals in two sandstone reservoir rocks. Minerals existing in these reservoir rocks were: quartz, albite, illite, montmorillonite and calcite. The sandstone reservoir rocks were denoted by SRR#1 and SRR#2, respectively. Moreover, PSR/mineral mixtures were created to estimate the effect of increasing calcite content and surface area. For understanding the impact of the surface area on the wettability, mineral mixtures were obtained by increasing the desired mineral content in the Sandstone Reservoir Rock#1. In other words, PSR#1 and PSR#2 were prepared by replacing 25% and 50% in SRR#1 rock mass with the illite, respectively. A similar method was applied to designing PSR#3 and PSR#4, but the altering mineral was calcite instead of the illite. The mineralogical composition of the sandstone reservoir rocks (SRR) and mineral mixtures are given in Table 3.1. The weight of the individual minerals and reservoir rocks was set to 0.2 g in each simulation. Reservoir temperature and pressure were assumed to be 90°C and 1 bar, respectively.

Minerals	*SRR#1*	*SRR#2*	*PSR#1*	*PSR#2*	*PSR#3*	*PSR#4*
Quartz	83.3	94.9	62.8	41.9	62.8	41.9
Albite	3.3	4.0	2.5	1.6	2.5	1.6
Montmorrolite	3.9	0.0	2.9	1.9	2.9	1.9
Illite	8.8	0.4	31.6	54.4	6.6	4.4
Siderite	0.0	0.5	0.0	0.0	0.0	0.0
Calcite	0.3	0.2	0.2	0.2	25.2	50.2

Table 3. 1: Mineralogical composition (weight percent) of the reservoir rocks and the mineral mixtures.

3.2 Properties of Stock Tank Oil and Brine Types

Properties of stock-tank oil (STO) and ionic composition of the synthetic FW employed in this study are given in Tables 3.2 and 3.3, respectively.

Fluid	Density (g/cm^3) at 20°C	TAN (mg KOH/g oil)	TBN (mg KOH/g oil)
STO#1	0.86	0.10	1.90
STO#2	0.90	0.38	2.30

Table 3. 2: Density, TAN, and TBN of STOs.

Ion	FW#1 (mmol/L)	FW#2 (mmol/L)
Na^+	1326.26	701.88
K^+	5.62	7.11
Mg^{2+}	17.46	23.90
Ca^{2+}	147.94	72.85
Sr^{2+}	8.44	1.65
Ba^{2+}	0.00	0.04
Cl^-	1677.67	898.69
SO_4^{2-}	0.89	3.59
Density(g/cm^3) at 20°C	1.07	1.04

Table 3. 3: Ionic compositions of the brines.

Two different CW solutions were prepared and applied in this study for a better understanding of the wettability alteration of the individual minerals, sandstone reservoir rocks (SRR#1 and SRR#2) and pseudo sandstone rock/mineral mixtures (PSR#1, PSR#2, PSR#3 and PSR#4) during CWI. Carbonated water (CW#1 and CW#2) was obtained by dissolving the 2 mmol/l of carbon gas into the ionic composition of synthetic formation water (FW#1 and FW#2) (Table 3.4). The temperature and pressure at which CW was formed were 90°C and 300 bar, respectively.

Ion	CW#1 (mmol/L)	CW#2 (mmol/L)
Na^+	1326.26	701.88
K^+	5.62	7.11
Mg^{2+}	17.46	23.90
Ca^{2+}	147.94	72.85
Sr^{2+}	8.44	1.65
Ba^{2+}	0.00	0.04
Cl^-	1677.67	898.69
SO_4^{2-}	0.89	3.59
$\boldsymbol{CO_3^{2-}}$	**2**	**2**
Density(g/cm^3) at 20°C	1.07	1.04

Table 3. 4: Ionic compositions of the carbonated waters.

3.3 The Electrostatic Pair Linkages

The attractive electrostatic forces between the oil-brine and the rock-brine interfaces result in the oil adhesion is defined by Bond Product (BP) [69]. The BP is represented as the product of the multiplied mole fraction of the differently charged oil (O_i) and mineral (n_i) sites:

$$BP = O_i n_i \tag{3.1}$$

TBP is the sum of all BP for a given mineral or rock. With the help of the TBP, the wettability state is defined by predicting oil's tendency to be adsorbed onto the mineral surface in SCM. In Figure 3.1, ">" and "<" represent the mineral and oil surface groups, respectively.TBP is defined as:

$$\text{TBP} = \sum_i^n BP_i \tag{3.2}$$

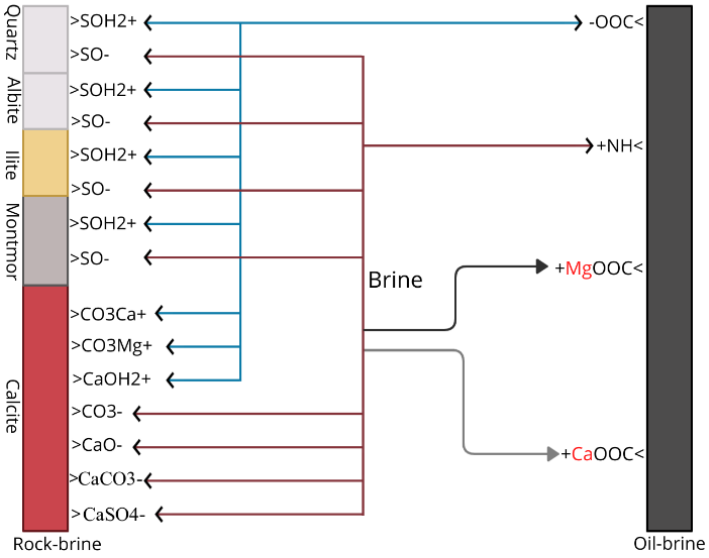

Figure 3. 1: The electrostatic pair linkages existing between the rock-brine and oil-brine interfaces with unlike charges.

In the dominant electrostatic pair linkages, oil adsorption on mineral can occur by different mechanisms: direct adsorption of carboxylate ($>COO^-$) onto the positive mineral sites ($>SOH_2^+$, $>CO_3Ca^+$, $>CO_3Mg^+$, $>CaOH_2^+$) and by bridging carboxylate ($>COO^-$) and negative mineral surfaces ($>SO^-$, $>CO_3^-$, $>CaO^-$, $>CaCO_3^-$, $>CaSO_4^-$) by divalent cations (Ca^{2+} and Mg^{2+}).

Mineral and oil surfaces dissociate when they contact brine, and dissociation and interaction between the dissociated surface and ions from the brine leads to a surface charge and potential generation. Table 3.5 illustrates surface reactions and reaction parameters that were used in the model. The surface charge was solved by the sum of the various surface complexes formed by the reactions. The surface potential was estimated from the surface charge with a diffuse-layer model.

3.4 The SCM Input Parameters

In crude oil, surface-active components are divided into acidic ($>COOH^-$) and basic ($>NH^+$) oil groups. The minerals are also represented by their respective mineral site (>Si-O-H, $>CO_3H$, and >CaOH). The surface reactions of oil and their reaction constants were taken from Brady and Krumhansl's paper, where similar reactions were performed [70]. The surface area and site

densities for quartz and albite were given by Sverjensky and Sahai [71], while enthalpy was obtained from similar kaolinite reactions [72]. For the illite and montmorillonite, the surface area and site densities were obtained from Gu and Evans [73] and Wieland et al. [74]. Also, the temperature-dependent reaction constants for illite and montmorillonite were taken from a similar reaction for kaolinite [72]. The surface area, site density, and reaction constants of the calcite were gained from Hjuler and Fabricius [75], Wolthers et al. [76], and Van Capellen et al. [77], respectively.

Reaction	Log K at 20°C	Enthalpy (kJ/mol)
Oil surface [a]		
$>NH^+ \leftrightarrow >N + H^+$	-6.0	34.0
$>COOH \leftrightarrow >COO^- + H^+$	-5.0	0.0
$>COOH + Ca^{2+} \leftrightarrow >COOCa^+ + H^+$	-3.8	1.2
$>COOH + Mg^{2+} \leftrightarrow >COOMg^+ + H^+$	-4.0	1.2[g]
Quartz [b]		
$>Si\text{-}O\text{-}H + H^+ \leftrightarrow Si\text{-}O\text{-}H_2^+$	-1.1	-26.4
$>Si\text{-}O\text{-}H \leftrightarrow Si\text{-}O\text{-} + H^+$	-8.1	8.4
Albite [c]		
$>Si\text{-}O\text{-}H + H^+ \leftrightarrow Si\text{-}O\text{-}H_2^+$	1.9	-26.4
$>Si\text{-}O\text{-}H \leftrightarrow Si\text{-}O\text{-} + H^+$	-8.5	8.4
Illite [d]		
$>Si\text{-}O\text{-}H + H^+ \leftrightarrow Si\text{-}O\text{-}H_2^+$	7.43	24.3[h]
$>Si\text{-}O\text{-}H \leftrightarrow Si\text{-}O\text{-} + H^+$	-8.99	18.8[i]
$H^+ + NaX_{ill} \leftrightarrow HX_{ill} + Na^+$	1.58	
Montmorrolite [e]		
$>Si\text{-}O\text{-}H + H^+ \leftrightarrow Si\text{-}O\text{-}H_2^+$	5.4	0
$>Si\text{-}O\text{-}H \leftrightarrow Si\text{-}O\text{-} + H^+$	-6.7	32
$H^+ + NaX_m \leftrightarrow HX_m + Na^+$	4.6	
Calcite [f]		
$>CO_3H \leftrightarrow >CO_3^- + H^+$	-4.9	-5.0
$>CO_3H + Ca^{2+} \leftrightarrow >CO_3Ca^+ + H^+$	-2.8	25.7
$>CO_3H + Mg^{2+} \leftrightarrow >CO_3Mg^+ + H^+$	-2.2	4.5
$>CaOH + H^+ \leftrightarrow >CaOH_2^+$	12.2	-77.5
$>CaOH \leftrightarrow >CaO^- + H^+$	-17.0	116.4
$>CaOH + 2H^+ + CO_3^{2-} \leftrightarrow >CaHCO_3 + H_2O$	24.2	-90.7
$>CaOH + CO_3^{2-} + H^+ \leftrightarrow >CaCO_3^- + H_2O$	15.5	-61.6
$>CaOH + SO_4^{2-} + H^+ \leftrightarrow >CaSO_4^- + H_2O$	13.9	-72.0

[a] after Brady and Krumhansl [70]

[b] and [c] after Sverjensky and Sahai [71], [72]

[d] after Gu and Evans [73]

[e] after Wieland et al. [74]

[f] after Wolthers et al. [76]

[g] enthalpy during Mg^{2+} reaction with >COOH was assumed to be the same as that of Ca^{2+}

[h] and [i] assumed to be the same as similar reactions as kaolinite

Table 3. 5: SCM input parameters.

The surface reactions and reaction constants of the minerals were utilized for reservoir rocks and mineral mixtures. Besides, the effective surface area (A_{eff}) of the rock (mineral mixture) was used as input into the SCM, and it is given by the relation:

$$A_{eff} = \sum_{n=1}^{\infty} m_i A_i \tag{3.3}$$

Where:

A_{eff} = Effective surface area (m^2/g)

m_i = Mass fraction of mineral I (dimensionless)

A_i = Intrinsic surface area of mineral I (m^2/g)

For the STO, site density was obtained by converting the Total Acid Number (TAN) and Total Base Number (TBN) of the STO into their respective organic acid and base component with the assumption that the surface area of the oil is the same as its respective mineral surface. The TAN/TBN were converted to their respective oil site density using:

$$\text{Oil-site density (site/nm}^2) = \frac{\text{TAN or TBN } (\text{mg}\frac{\text{KOH}}{\text{g}}\text{oil})}{\text{Mw KOH}\left(\frac{\text{g}}{\text{mol}}\right)} \times \frac{\text{Avogadro's number}}{\text{Surface area } (\frac{\text{m2}}{\text{g}})} \tag{3.4}$$

where Mw is the molecular weight. The intrinsic properties of minerals/rocks, such as site densities and the effective surface area, and STO estimated site density are given in Table 3.6 and 3.7, respectively.

All these simulations were performed with the geochemistry solver PHREEQ-C [78]. PHREEQ-C is mainly utilized in groundwater chemistry and is increasingly used to perform reactions in the oil reservoir. It can simulate various reactions such as mineral equilibrium in brine, brine speciations, mineral-reaction kinetics, electromigration, and surface complexation.

Surface	*Site Density (site/nm²)*	*Surface Area (m²/g)*
Quartz	10.00	1.20
Albite	1.155	1.20
Illite	1.37	66.8
Montmorrolite	5.7	3.0
Calcite	4.90	2.00
Kaolinite	1.16	10.0
SRR#1		7.0
SRR#2		1.5
PSR#1		22.0
PSR#2		36.9
PSR#3		5.8
PSR#4		4.5

Table 3. 6: Properties of minerals and reservoir rocks.

Surface	*Oil Site*	*STO#1 Site Density (site/nm^2)*	*STO#2 Site Density (site/nm^2)*
Quartz	>COOH	0.89	3.40
	>NH$^+$	16.99	20.56
Albite	>COOH	0.89	3.40
	>NH$^+$	16.99	20.56
Illite	>COOH	0.02	0.06
	>NH$^+$	0.31	0.37
Montmorillonite	>COOH	0.36	1.36
	>NH$^+$	6.79	8.23
Calcite	>COOH	0.54	2.04
	>NH$^+$	10.20	12.34
Kaolinite	>COOH	0.10	0.41
	>NH$^+$	2.04	2.47
SRR#1	>COOH	0.15	0.58
	>NH$^+$	2.89	3.50
SRR#2	>COOH	0.73	2.77
	>NH$^+$	13.85	16.76
PSR#1	>COOH	0.05	0.19
	>NH$^+$	0.93	1.12
PSR#2	>COOH	0.03	0.11
	>NH$^+$	0.55	0.67
PSR#3	>COOH	0.19	0.70
	>NH$^+$	3.52	4.27
PSR#4	>COOH	0.24	0.90
	>NH$^+$	4.51	5.46

Table 3. 7: Estimated oil site densities of the STO used.

4 Results

The SCM was used to estimate the wettability by evaluating the oil-adhesion tendencies caused by the electrostatic pair linkages during rock/brine/oil interactions. The results obtained from simulations with FW and CW for minerals were presented to investigate the alteration wetting preferences of individual minerals during CWI. Besides, the oil-brine and mineral-brine interactions that led to the adhesion of oil onto the mineral surfaces were also assessed via SCM. Only the most dominating interactions were shown in the plots, as less essential interactions have minimal effect on the wettability preferences of the mineral. Afterward, the same procedures were done for reservoir rocks and mineral mixtures (SRR and PSR). Erzuah et al. [62] performed the same type of simulations for rock/mineral in FW in their work, which was given in Chapter 2.5.

4.1 Minerals

4.1.1 Total Bond Product

i. Formation water

The SCM can characterize wettability by estimating the tendency of oil to be adhered to a surface using TBP. Figure 4.1 represents the TBP for each mineral during Formation Water Injection (FWI). From the SCM results, it can be concluded that quartz is strongly water-wet (max TBP < 0.1), while calcite is strongly oil-wet (min TBP > 0.8). On the other hand, montmorillonite is more hydrophobic than illite, albite, and quartz. Hence, the increasing order of the mineral hydrophobicity is given as quartz < albite < illite < montmorillonite < calcite.

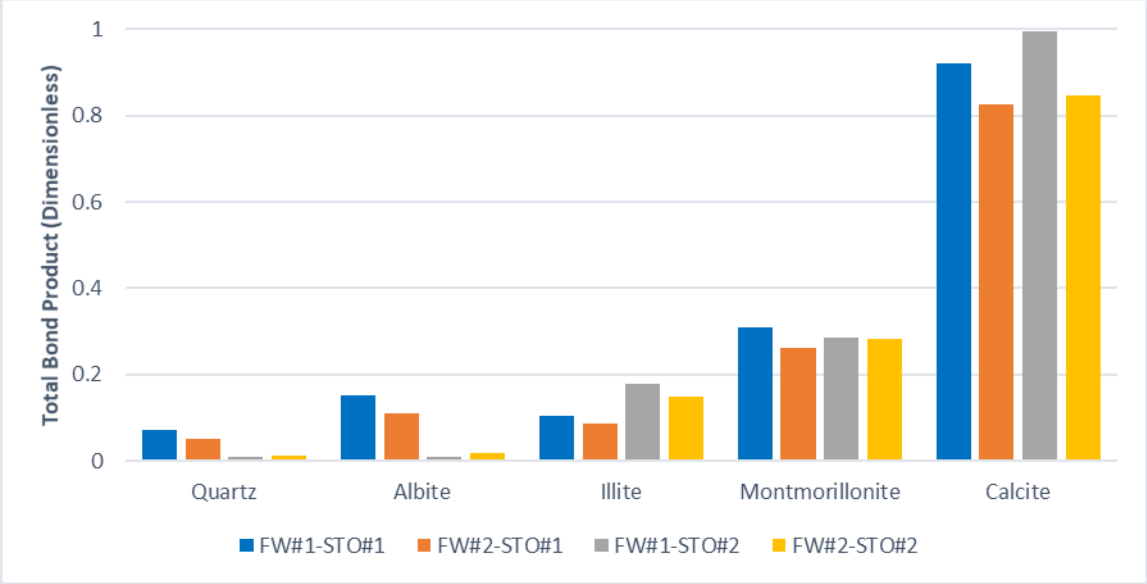

Figure 4. 1: Prediction of the oil-adhesion tendencies of minerals using the total bond product during FWI.

ii. Carbonated water

After applying CW instead of FW, some alterations in the minerals' TBP can be observed. The results in Figure 4.2 illustrate that calcite is not acting as strong oil-wet anymore (max TBP < 0.4), and other minerals are more hydrophilic compare to results with FW (Figure 4.1). The increasing order of the mineral hydrophobicity also changed slightly, where illite and montmorillonite swapped their places; quartz < albite < montmorillonite < illite < calcite.

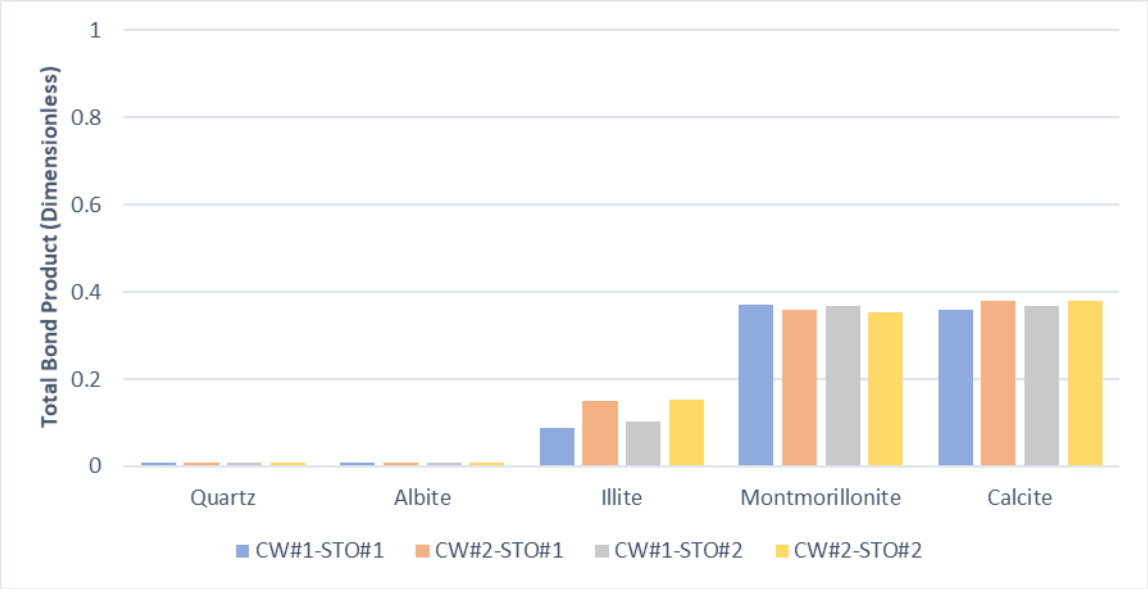

Figure 4. 2: Prediction of the oil-adhesion tendencies of minerals using the total bond product during CWI.

4.1.2 Mechanisms of Oil Adhesion in Quartz

i. Formation water

Figure 4.3 demonstrates that during FWI, quartz can be considered a strongly water-wet as all BPs are less than < 0.1. For quartz, the most dominant attractive electrostatic pair linkage exists between $>SO^-$ and $>COOCa^+$ and the least dominant electrostatic pair linkage is between $>SiO^-$ and $>NH^+$. It can be explained by the fact that the carboxylic acidic components of the STO have a more intense effect on the wetting parameters than the basic components. It can be noticed that two negatively charged surfaces are bridged by divalent cations (Ca^{2+}, Mg^{2+}) in oil-brine and quartz-brine interactions.

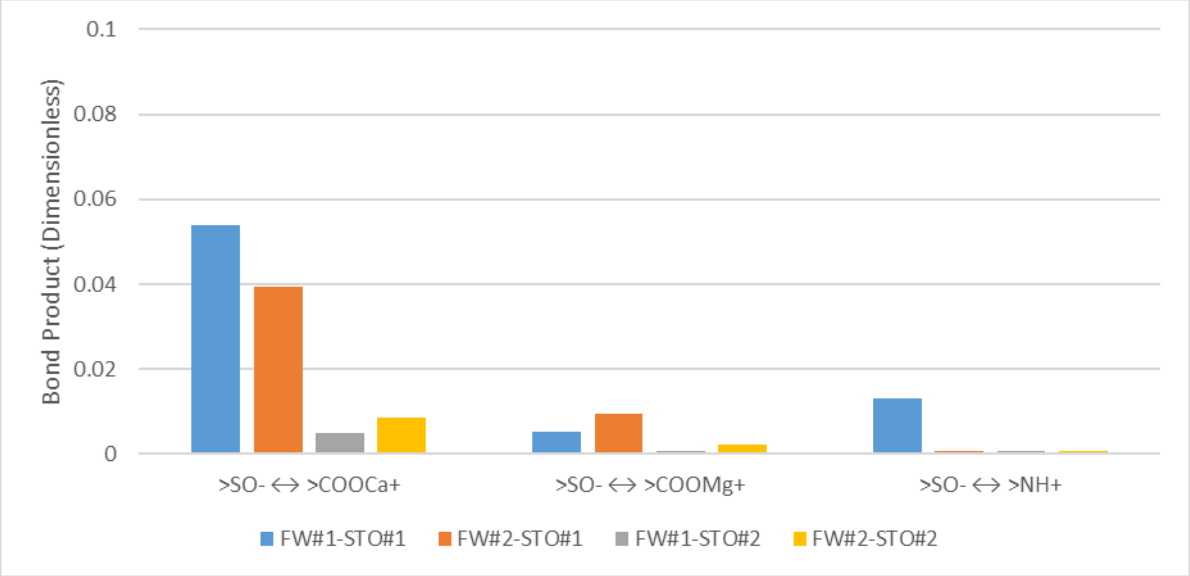

Figure 4. 3: Prediction of the oil-adhesion tendency of quartz using the bond product during FWI.

ii. Carbonated water

The results presented in Figure 4.4 give evidence that CWI decreases the electrostatic pair linkage in oil-brine and quartz-brine interactions (max BP ≈ 0) and oil's tendency to be adhered onto a surface. In addition, these reductions contribute to an increase in mineral hydrophilicity.

Figure 4. 4: Prediction of the oil-adhesion tendency of quartz using the bond product during CWI.

4.1.3 Mechanism of Oil Adhesion in Albite

i. Formation water

From Figure 4.5, albite can also be considered as a water-wet mineral like quartz. However, compared with quartz, albite is less hydrophilic as dominant BP between $>SO^-$ and $>COOCa^+$ is more than > 0.1. The interactions in the albite-brine and oil-brine interfaces are dominated by divalent cations (Ca^{2+}, Mg^{2+}) bridging. Similar to quartz, the electrostatic pair linkage between the acidic component of the oil and the mineral surface significantly contributes to the oil adhesion mechanism in albite.

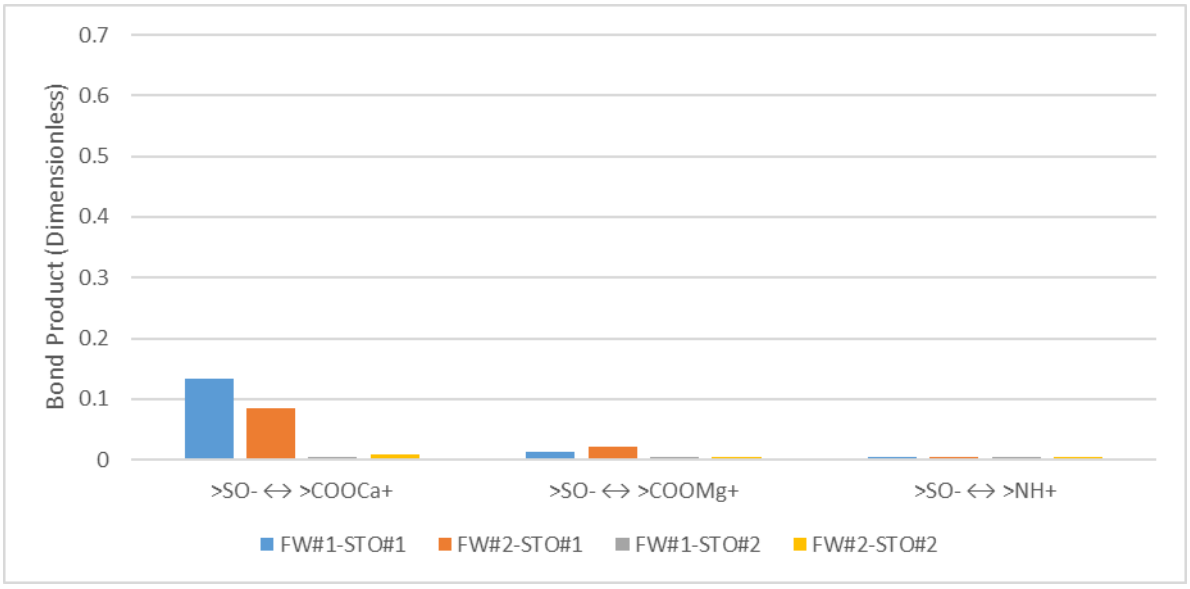

Figure 4. 5: Prediction of the oil-adhesion tendency of albite using the bond product during FWI.

ii. Carbonated water

It can be observed from Figure 4.6 that, after applying CW instead of FW like in quartz, the albite wettability preferences alter towards more hydrophilic as the BP for the dominant electrostatic pair linkages decrease sharply (max BP ≈ 0).

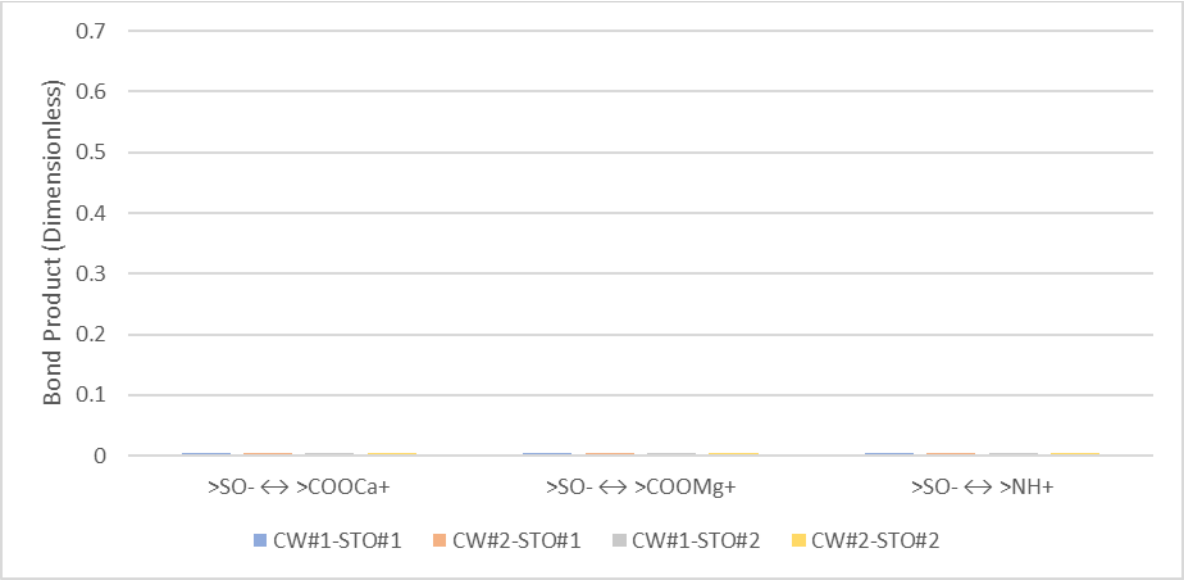

Figure 4. 6: Prediction of the oil-adhesion tendency of albite using the bond product during CWI.

4.1.4 Mechanism of Oil Adhesion in Illite

i. Formation water

From Figure 4.7, it can be seen that illite in FW is more oil-wet (max BP ≈ 0.2) than albite and quartz (max BP ≈ 0.1 and max BP < 0.1, respectively). Moreover, as opposed to quartz and albite, in oil-brine and illite-brine interactions, dominant electrostatic pair linkage is between carboxylate ($>COO^-$) and positive illite surface ($>SOH_2^-$). Besides, bridging of negative oil and mineral surfaces by divalent cations such as Ca^{2+} and Mg^+ also occur in these interactions. Similar to previously mentioned minerals (quartz, albite), contributions from basic oil components are also negligible compared to acidic components.

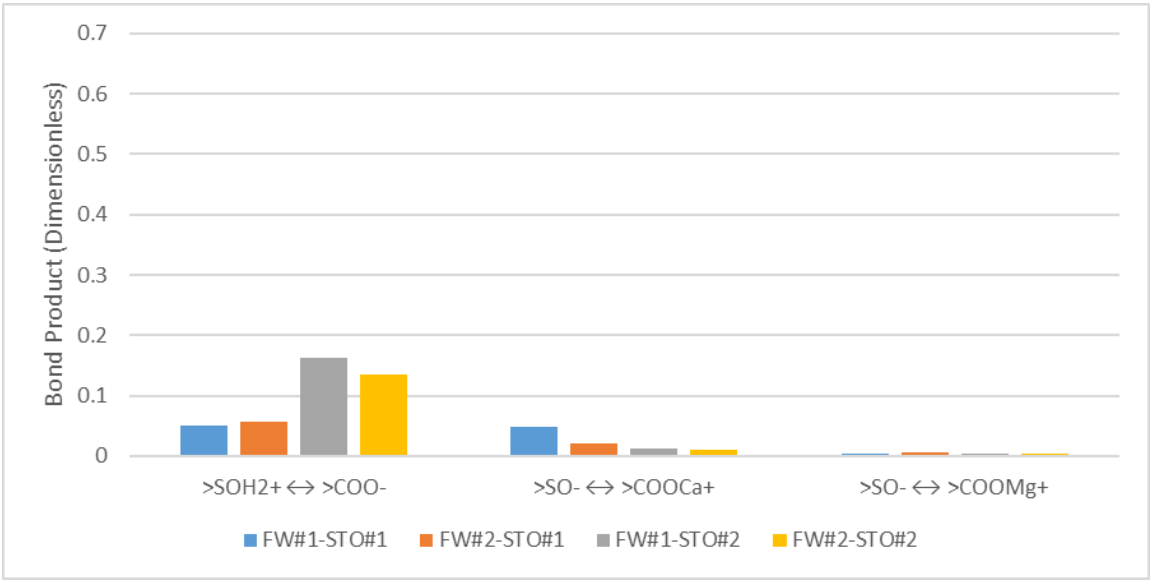

Figure 4. 7: Prediction of the oil-adhesion tendency of illite using the bond product during FWI.

ii. Carbonated water

It can be observed from Figure 4.8 that the wettability state of illite is slightly altered after using CW towards more water-wet (max BP < 0.15) compared to previous results with FW (max BP ≈ 0.2). The interactions in the albite-brine and oil-brine interfaces are still dominated by direct adhesion of carboxylate ($>COO^-$) onto the positive illite surface. In contrast, BPs for less dominant oil adhesion mechanisms (by divalent cations) decreases drastically, contributing to the wettability alteration of illite toward more hydrophobic.

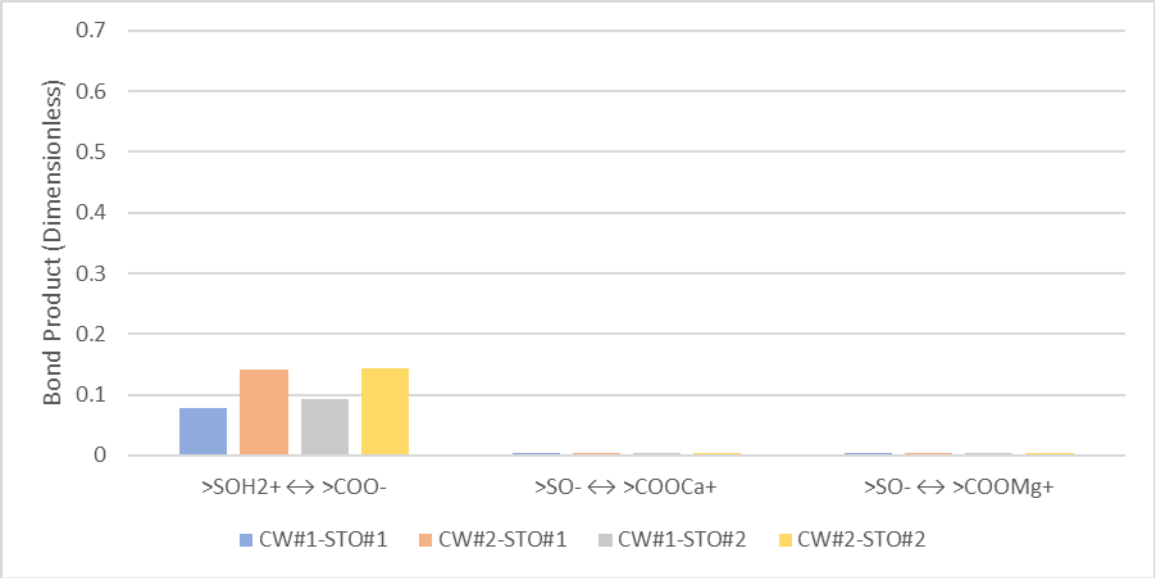

Figure 4. 8: Prediction of the oil-adhesion tendency of illite using the bond product during CWI.

4.1.5 Mechanism of Oil Adhesion in Montmorillonite

i. Formation water

From Figure 4.9, it can be seen that montmorillonite in FW (max BP ≈ 0.25) is less hydrophilic than illite (max BP ≈ 0.2), albite (max BP ≈ 0.1), and quartz (max BP < 0.1). The dominant electrostatic pair linkage in the oil adhesion mechanism on the mineral is cation bridging (Ca^{2+}, Mg^{2+}), similar to albite and quartz. Also, in oil adhesion onto montmorillonite, the contribution of the basic components ($>NH^+$) in the oil is insignificant as compared to the acidic component ($>COO^-$).

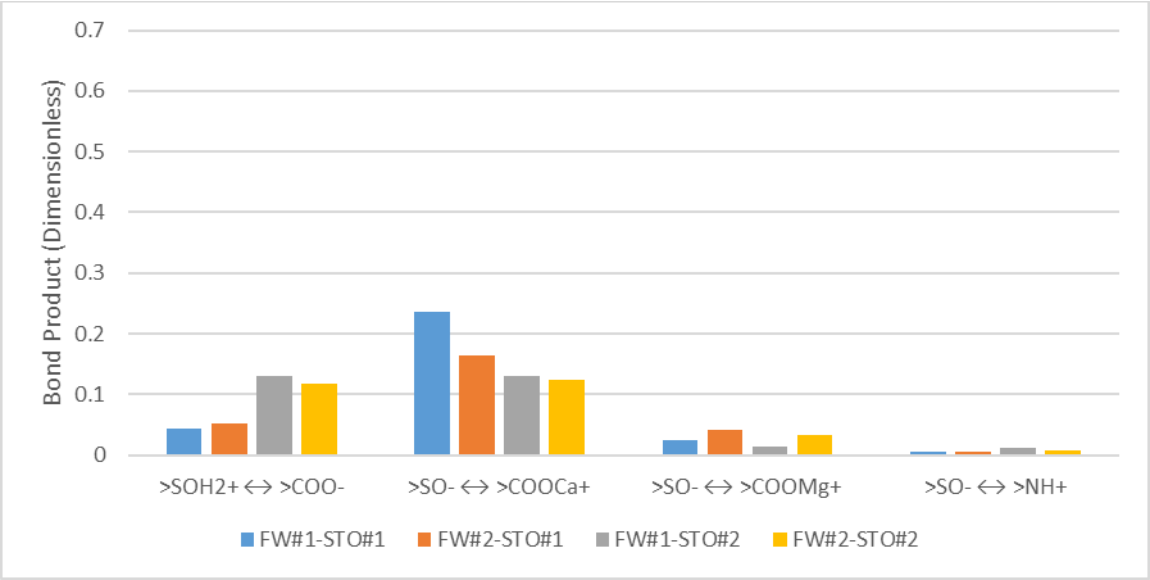

Figure 4. 9: Prediction of the oil-adhesion tendency of montmorillonite using the bond product during FWI.

ii. Carbonated water

It can be observed from Figure 4.10 that, after applying CW instead of FW, the dominant electrostatic pair linkage between oil-brine and montmorillonite-brine interactions alter from the cation bridging mechanism (Ca^{2+}, Mg^{2+}) to direct adhesion of carboxylate ($>COO^-$) onto the positive mineral surface ($>SOH_2^+$). Besides, the basic component ($>NH^+$) contribution in the oil becomes significant in the oil adhesion mechanism. These changes in the oil adhesion mechanism contribute wettability state of montmorillonite switch toward less water-wet. Even Figure 4.10 illustrates that BP for non-dominant electrostatic pair linkages ($>SO^- \leftrightarrow >COOCa^+$ and $>SO^- \leftrightarrow >COOMg^+$) remarkably decrease (max BP ≈ 0).

Figure 4. 10: Prediction of the oil-adhesion tendency of montmorillonite using the bond product during CWI.

4.1.5 Mechanism of Oil Adhesion in Calcite

i. Formation water

It can be observed from Figure 4.11 that the wettability preferences of the calcite in FW are toward strong oil-wet as the BP for the dominant electrostatic pair linkages ($>CaOH_2^+ \leftrightarrow >COO^-$) is more significant than 0.4 ($\approx 0.43 - 0.63$) compared to montmorillonite (max BP $\approx$ 0.25), illite (max BP $\approx$ 0.2), albite (max BP $\approx$ 0.1), and quartz (max BP < 0.1). The direct adhesion of carboxylate ($>COO^-$) onto a positively charged calcite site also occurs, like in montmorillonite ($>SOH_2^+$) and illite ($>SOH_2^+$). Nevertheless, BP for calcite ($>CaOH_2^+ \leftrightarrow >COO^-$) is higher than illite and montmorillonite ($>SOH_2^+ \leftrightarrow >COO^-$), estimating the mineral's hydrophobic nature. In addition, the cation bridging by divalent cations (Ca^{2+}, Mg^{2+}) also takes place in oil adhesion mechanisms onto calcite like in other minerals (quartz, albite, illite, montmorillonite). One more similarity with previous mineral/brine/oil interactions is the insufficient effect of the basic component ($>NH^+$) in the oil adhesion mechanisms compared to the acidic component ($>COO^-$).

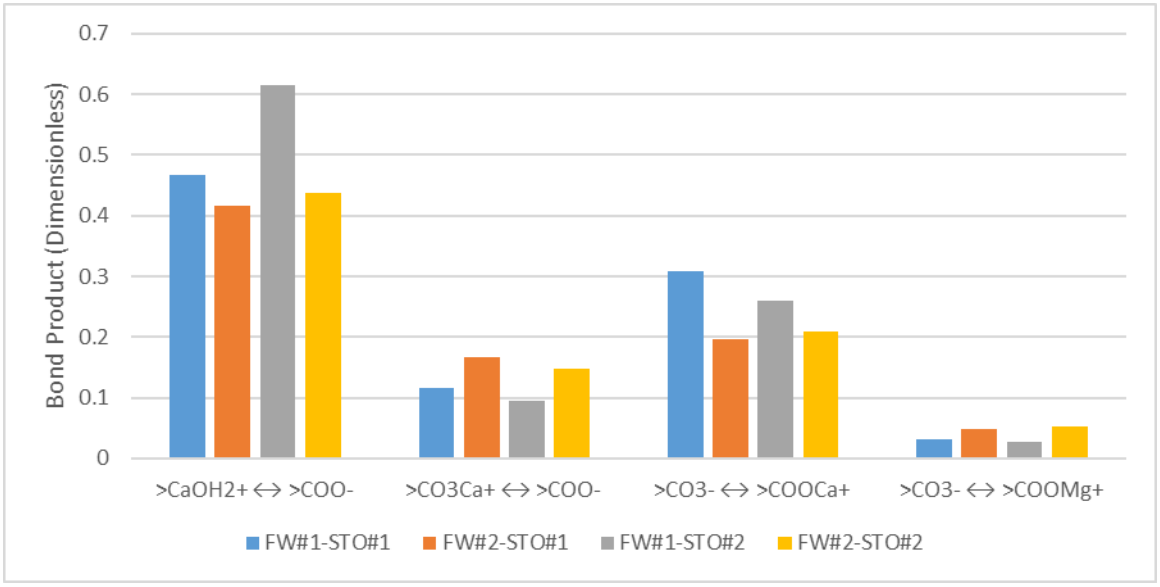

Figure 4. 11: Prediction of the oil-adhesion tendency of calcite using the bond product during FWI.

ii. Carbonated water

The difference between a BP for dominant electrostatic pair linkages before (max BP $\approx$ 0.6) and after (max BP $\approx$ 0.3) applying CW demonstrates the wettability alteration of calcite. In addition, the diminishing in the BPs leads calcite to become less hydrophobic (Figure 4.12).

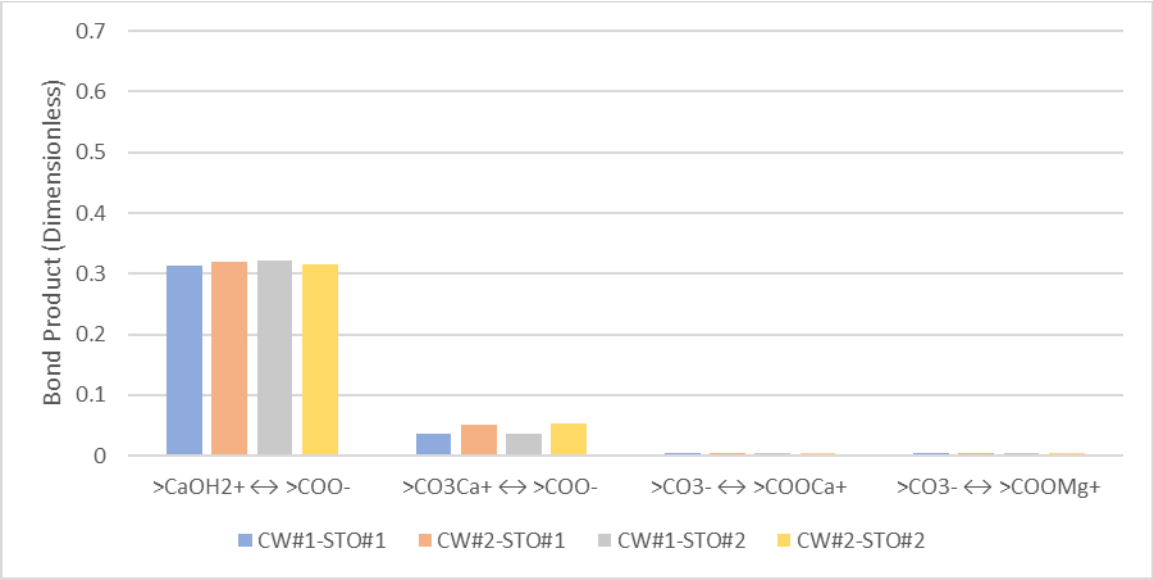

Figure 4. 12: Prediction of the oil-adhesion tendency of calcite using the bond product during CWI.

4.2 Reservoir Rock and Mineral Mixtures

4.2.1 Total Bond Product

i. Formation water

From Figure 4.13, it can be observed that the wettability preferences of the rocks are dictated by the surface area and wetting state of the individual minerals. The dominated mass fraction for PSR#1 is quartz (62.8%), while for PSR#2, it is illite (54.4%). As the wetting state of both quartz and illite were water-wet during FWI in the previous studies (Figure 4.1), naturally, the wetting preferences of PSR#1 and PSR#2 are similar to the wetting state of the mineral with the dominant effective surface area. Illite is also the dominant mineral in PSR#3 and PSR#4's effective surface area (4.40 m^2/g and 2.94 m^2/g, respectively). Nevertheless, in PSR#3, the dominant mass fractions are quartz (62.8%) and calcite (25.2%), while for PSR#4, these are calcite (50.2%) and quartz (41.9%). Even the surface area and the mass fraction are dominated by hydrophilic minerals (illite and quartz), the wettability state of PSR#3 is less water-wet than SRR#1 due to the higher content of calcite in PSR#3 than SRR#1. When coming to PSR#4, the dominant surface area is from illite, while the mass fraction of the PSR#4 is dominated by calcite which contributed to the wetting preferences of the mineral mixture toward more hydrophobic.

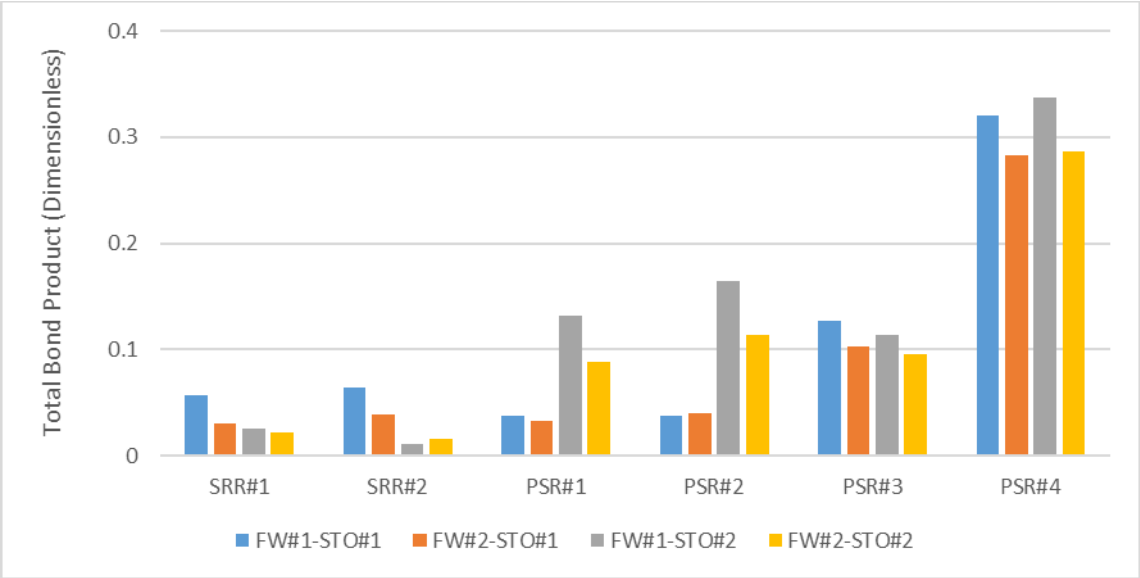

Figure 4. 13: Prediction of the oil-adhesion tendencies of reservoir rocks and mineral mixtures using the total bond product during FWI.

ii. Carbonated water

After applying CW, the wettability preferences of the reservoir rocks (SRR#1 and SRR#2) and mineral mixtures (PSR#1, PSR#2, PSR#3, PSR#4) alter individually for each rock. From Figure 4.13, it can be observed that the wettability preferences of SRR#1 become slightly more hydrophobic due to the surface area being dominated by illite, which has more vital BPs with positively charged oil surface after applying CW. A similar effect can be noticed in PSR#1 and PSR#2 because illite has the dominating surface area. While for SRR#2, wettability alters directly toward more water-wet during CWI. The main reason for this is that the dominating surface is from quartz. The wettability state of the quartz changes towards more hydrophilic during CWI at the studied conditions (Figure 4.4). For PSR#3 and PSR#4, the wettability states alter from oil-wet to water-wet because of the high content of calcite.

Figure 4. 14: Prediction of the oil-adhesion tendencies of reservoir rocks and mineral mixtures using the total bond product during CWI.

4.2.2 Mechanism of Oil Adhesion in SRR#1

i. Formation water

From Figure 4.15, it can be observed that the composition of the SRR#1 is dominated by quartz (83.7%). Besides, even though the illite content (8.8%) is small, it affects the rock wettability more than other minerals due to its large surface area, proving that minerals' intrinsic properties impose wettability.

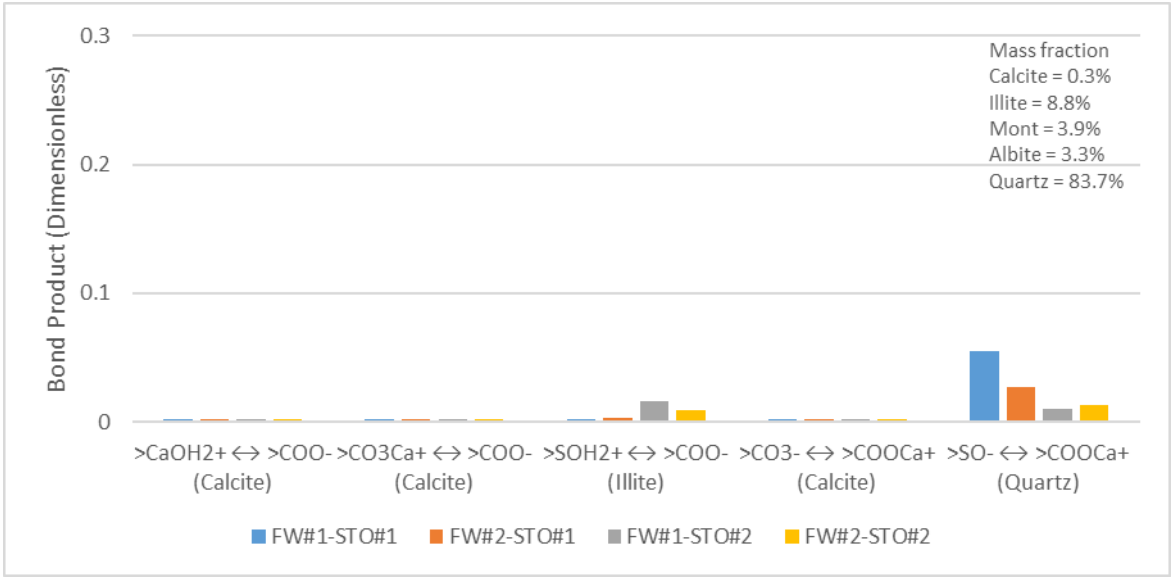

Figure 4. 15: Prediction of the oil-adhesion tendency of SRR#1 using the bond product during FWI.

ii. Carbonated water

After applying CW, TBP for electrostatic pair linkage between illite and oil interactions increases, which also can be observed in Chapter 4.1.4. Simultaneously, the dominant pair linkage between quartz and oil surfaces ($>SO^- \leftrightarrow >COOCa^+$) decreases, as explained in Chapter 4.1.2. (Figure 4.4). Alterations in individual minerals' BPs lead to wettability preferences of SRR#1 to change to more water-wet. From Figure 4.16, it can be seen that wettability alteration in SRR#1 is noticed due to changing wettability state of the individual minerals (mainly: quartz and illite) after applying CW.

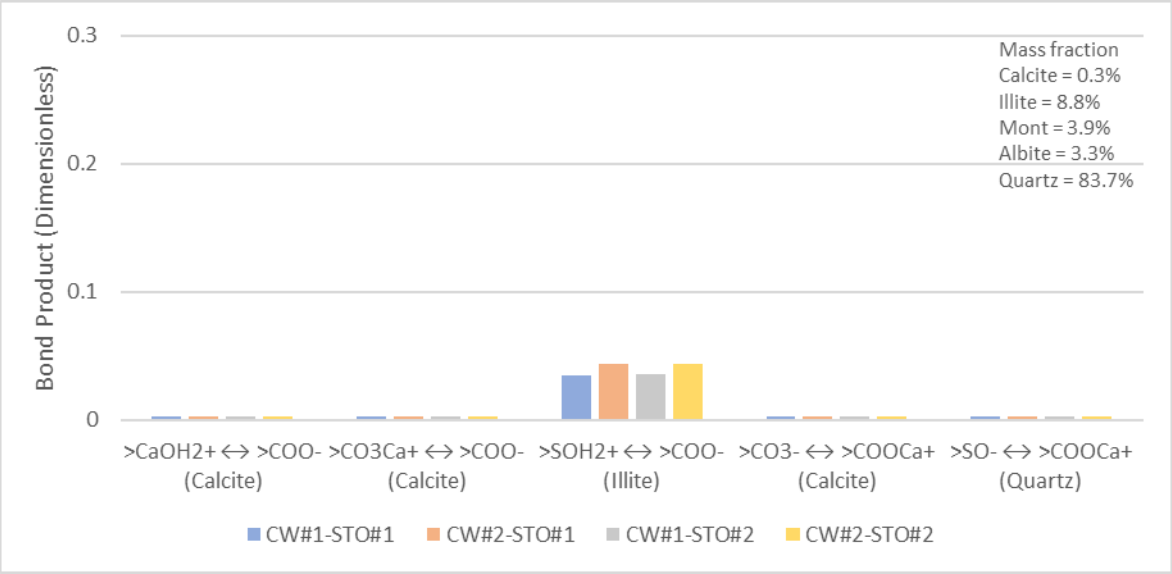

Figure 4. 16: Prediction of the oil-adhesion tendency of SRR#1 using the bond product during CWI.

4.2.3 Mechanism of Oil Adhesion in SRR#2

i. Formation water

Analogous to SRR#1 composition (Table 4.1) with high quartz content (83.7%), the composition of SRR#2 (Table 4.1) is also dominated by quartz (94.9%). Moreover, another similarity between SRR#1 and SRR#2 during FWI can be observed in electrostatic pair linkages between reservoir rock-brine and oil-brine interfaces where the highest BP number is less than 0.1 (max BP < 0.1) in both reservoir rocks (SRR#1 and SRR#2). However, Figure 4.17 shows that due to low illite content (0.4%), the BP for dominant electrostatic pair linkage between illite-brine and oil-brine ($>SOH_2^+ \leftrightarrow >COO^-$) is less than SRR#1 (Figure 4.15). In other words, unlike SRR#1, the effect of illite on the wettability preferences of the SRR#2 is negligible, which demonstrates that the effective surface area of the individual minerals constituting the reservoir rock has a significant effect on the wettability. The cation bridging (Ca^+) between two

negatively charged surfaces of quartz (>SO^-) and oil (>COO^-) is the dominant electrostatic pair linkage for oil adsorption onto the SRR#2. Besides, direct adsorption of carboxylate (>COO^-) onto the positive sites of the SRR#2 minerals (calcite and illite) also happens. Nevertheless, because of the less effective surface area of these minerals, their effect on the wettability of the rock is insignificant.

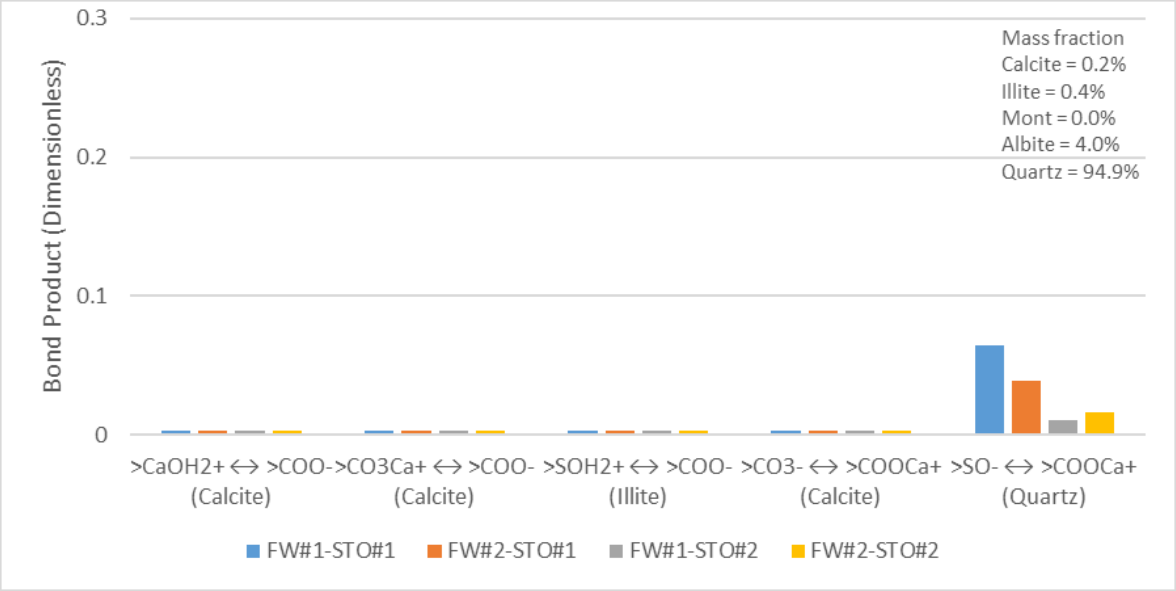

Figure 4. 17: Prediction of the oil-adhesion tendency of SRR#2 using the bond product during FWI.

ii. Carbonated water

Figure 4.18 illustrates the alteration of the electrostatic pair linkage between SRR#2-brine and oil-brine interactions after applying CW instead of FW. From previous results (Figure 4.4), it can be concluded that the wetting state of quartz becomes more hydrophilic (max BP ≈ 0) during CWI. Simultaneously, the past studies (Figure 4.8) show that illite has the opposite effect in this condition; still, the wettability alteration of illite is not noticeable in the results below. The main reason is the small effective surface area of illite, contributing to minor alteration of the BP. Overall, the wettability preferences of SRR#2 change toward more water-wet (max BP ≈ 0).

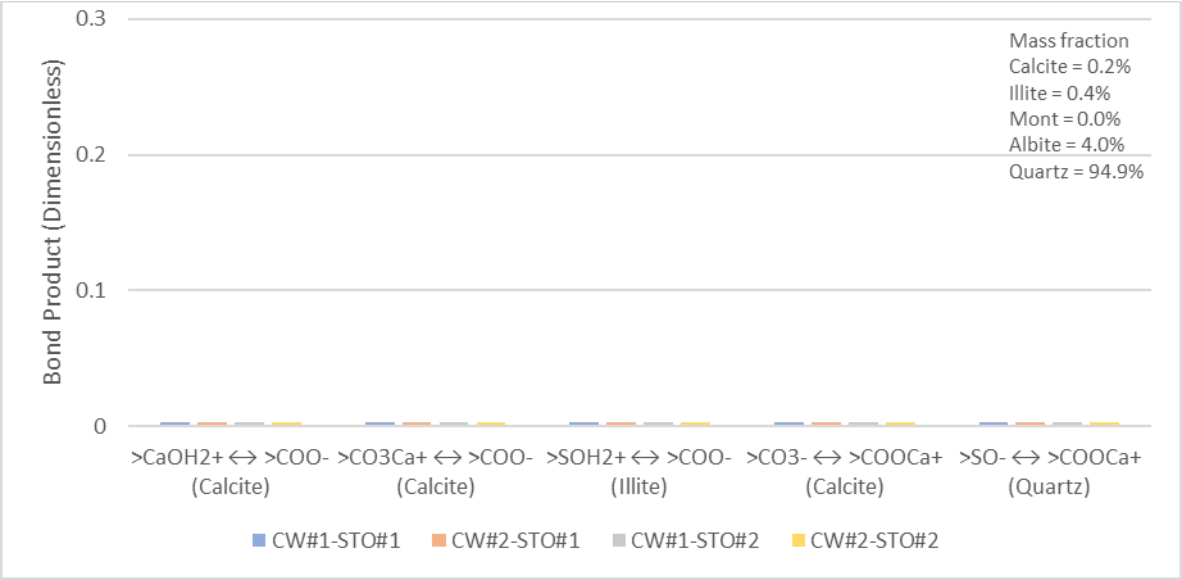

Figure 4. 18: Prediction of the oil-adhesion tendency of SRR#2 using the bond product during CWI.

4.2.4 Mechanism of Oil Adhesion in PSR#1 and PSR#2

i. Formation water

From Table 3.1, it can be observed that the main difference in the compositions of PSR#1 and PSR#2 from the sandstone reservoir rocks compositions (SRR#1 and SRR#2) is higher illite content (31.6% and 54.4%, respectively). The compositions of PSR#1 and PSR#2 were designed to understand better the effect of increasing surface area of the mineral mixture on wettability by adding illite. For PSR#1, the mass fraction of illite is 32%, and Figure 4.19 illustrates the electrostatic pair linkages between PSR#1-brine and oil-brine interactions. The dominant attractive electrostatic pair linkage during FWI in PSR#1 is the direct adhesion of the carboxylate ($>COO^-$) onto the positive illite surface ($>SOH^+$). Besides, the bridging by divalent cation (Ca^{2+}) between the negative oil ($>COO^-$) and quartz ($>SO^-$) surfaces has a minor effect on the wettability state of the PSR#1 (max BP < 0.05).

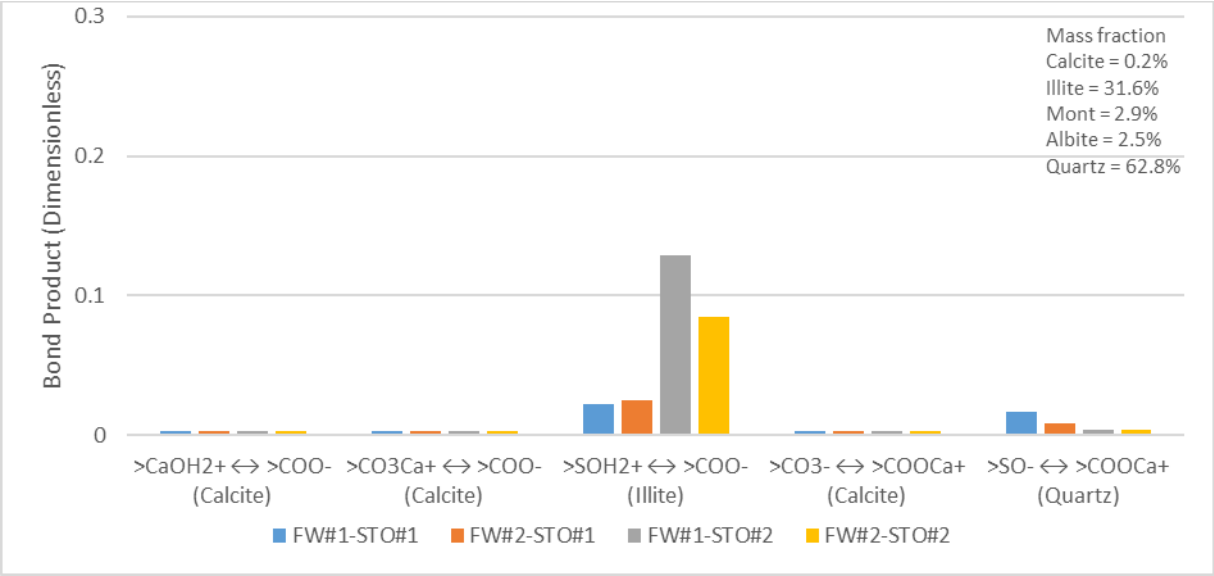

Figure 4. 19: Prediction of the oil-adhesion tendency of PSR#1 using the bond product during FWI.

From Figure 4.20, it can be seen that for PSR#2, the dominant attractive electrostatic pair linkage is the same as PSR#1 ($>SOH_2^+ \leftrightarrow >COO^-$). From Figure 4.19, it can be observed that even illite is the second dominant mineral (3.16%) in PSR#1 composition; its interactions are more vital than that of quartz (62.8%). Besides, From Figure 4.20, it can also be seen that even though quartz the second dominant mineral in PSR#2, quartz-brine and oil-brine interaction ($>SO^- \leftrightarrow >COOCa^+$) is not noticeable. This is related to its small surface area, thereby contributing to the insignificant effective surface area compared to illite. In other words, due to the large effective surface area, illite overshadows the contribution of the quartz.

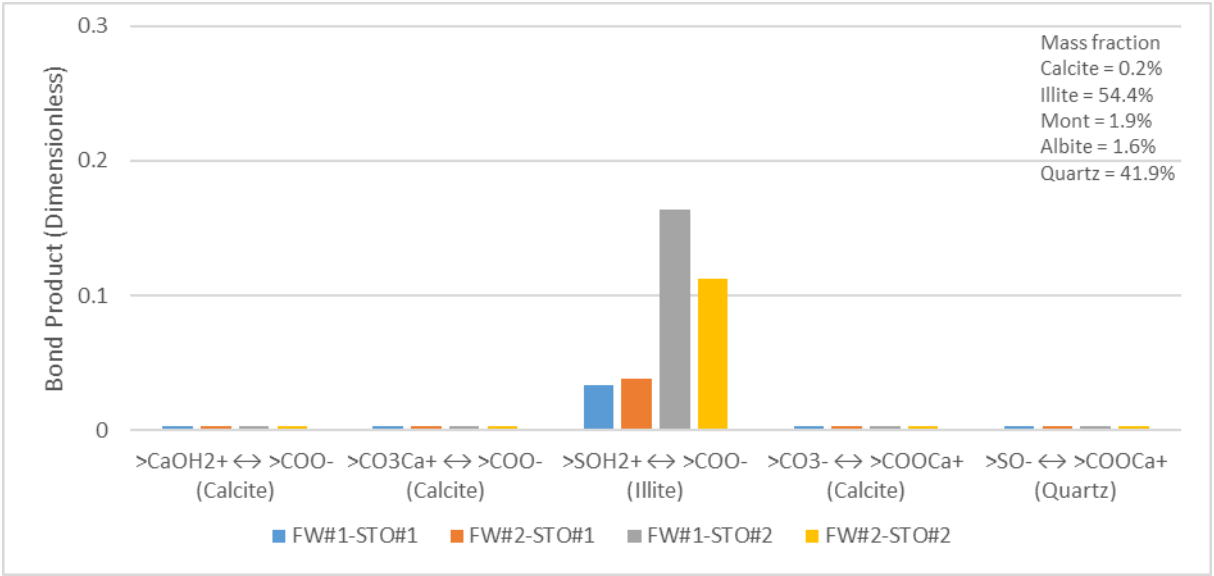

Figure 4. 20: Prediction of the oil-adhesion tendency of PSR#2 using the bond product during FWI.

ii. Carbonated water

As the dominant mineral in the effective surface area of the mineral mixtures (PSR#1 and PSR#2) is the illite, CW's effect on the wettability alteration is based on the previous study of this mineral (Figure 4.8).

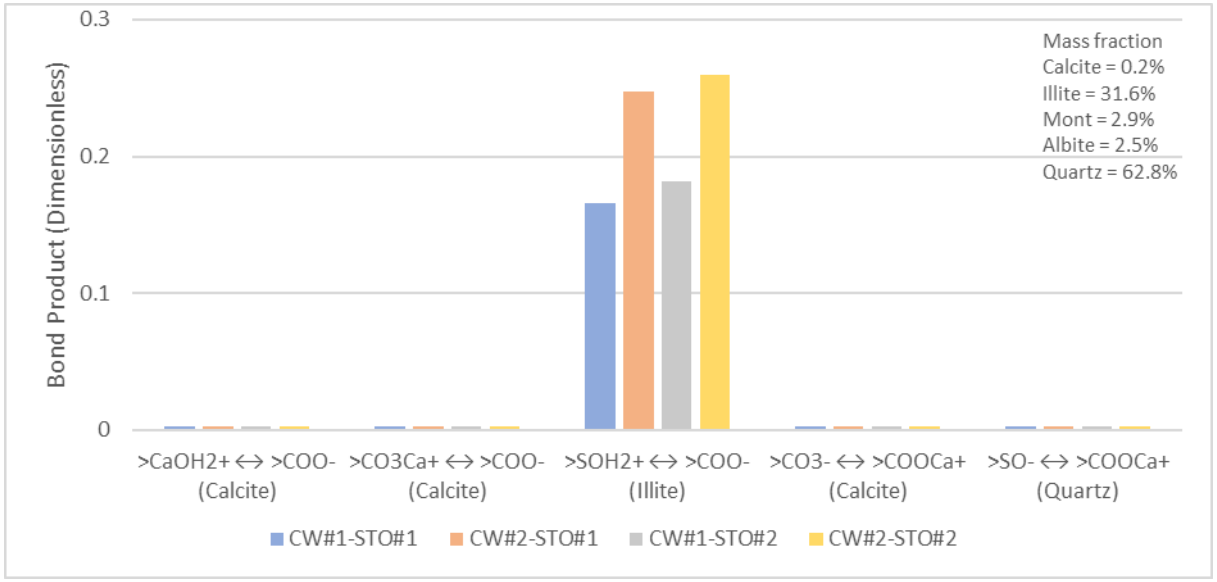

Figure 4. 21: Prediction of the oil-adhesion tendency of PSR#1 using the bond product during CWI.

Figure 4.21 and Figure 4.22 show that the direct adhesion of oil (COO^-) onto positively charged illite ($>SOH_2^+$) surface is dominant in mineral mixture-brine (PSR#1 and PSR#2) and oil-brine interactions (max BP > 0.2). Moreover, wettability preferences of both PSR#1 and PSR#2 are altered toward more hydrophobic during CWI.

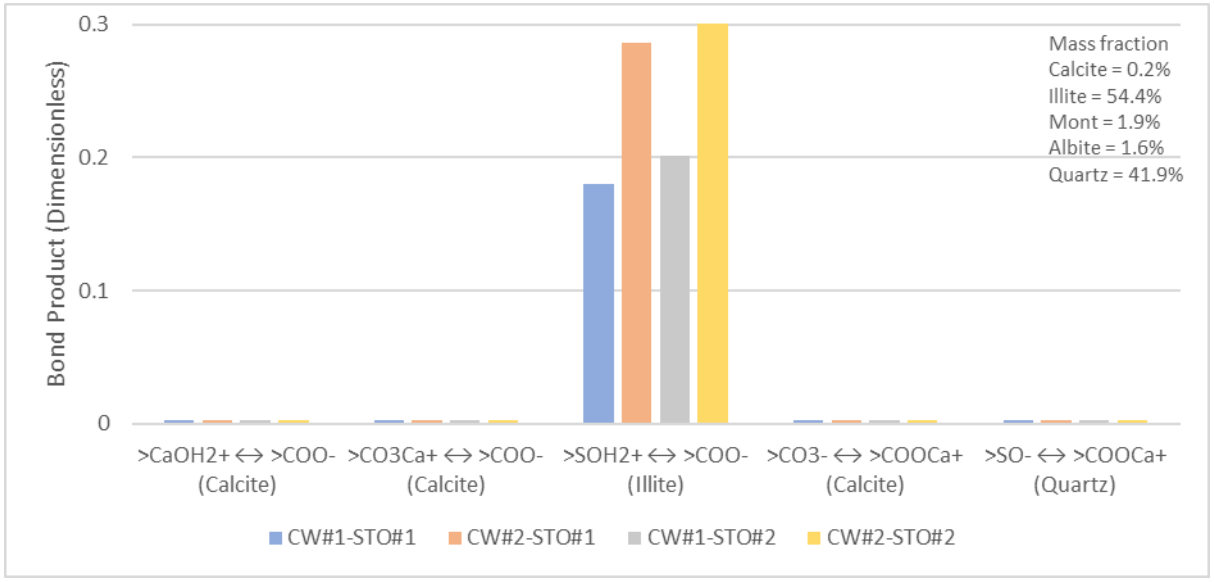

Figure 4. 22: Prediction of the oil-adhesion tendency of PSR#2 using the bond product during CWI.

4.2.5 Mechanism of Oil Adhesion in PSR#3 and PSR#4

i. Formation water

Unlike PSR#1 and PSR#2 with illite dominant contents (31.6% and 54.4%, respectively), PSR#3 and PSR#4 were designed to be dominated by calcite (25.2% and 50.2%, respectively), a more hydrophobic mineral. These mineral mixture compositions (PSR#3 and PSR#4) were created to understand the effect of increasing calcite content on the wettability preferences of the mineral mixtures (PSR#3 and PSR#4).

From Figure 4.23, it can be observed for PSR#3 that the dominant electrostatic pair linkage in the oil adhesion mechanism on the rock mineral is the direct adsorption of carboxylate ($>COO^-$) onto the positive calcite ($>CaOH^{2+}$) site (max BP < 0.1) during FWI.

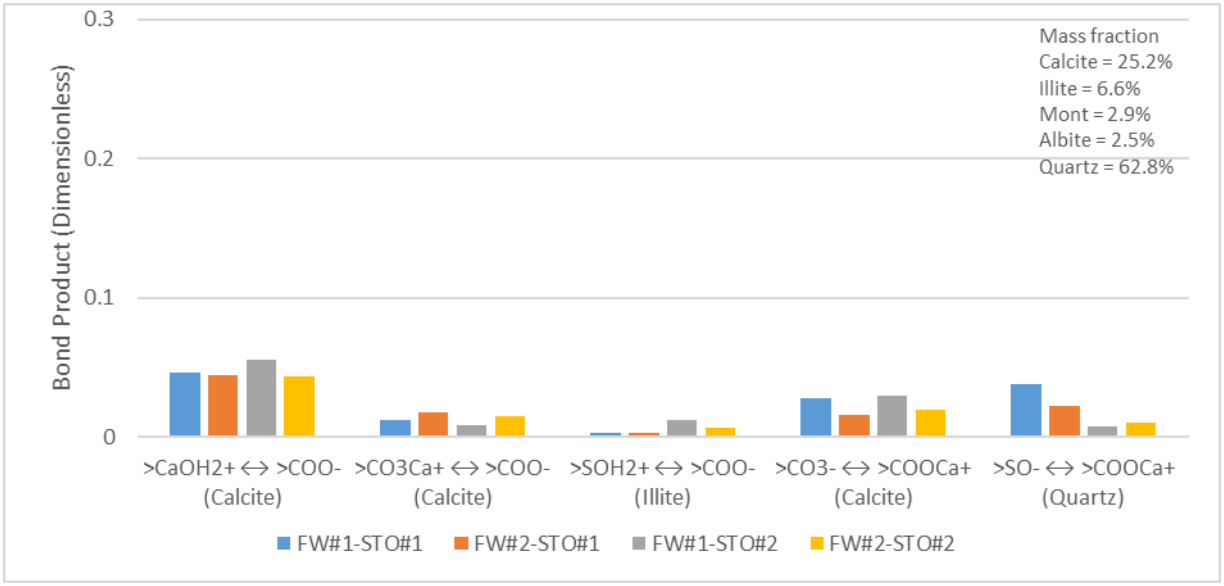

Figure 4. 23: Prediction of the oil-adhesion tendency of PSR#3 using the bond product during FWI.

Figure 4.24 shows that during FWI in PSR#4, the BP for the dominant pair linkages ($>CaOH_2^+ \leftrightarrow >COO^-$) is around 0.2, verifying that escalating the calcite content of the reservoir rock contributes to its wettability state toward more oil-wet. Figure 4.20 and Figure 4.24 show that with the same range of quartz (48,3%), the oil adhesion in PSR#4 (min BP > 0) is more significant than in PSR#2 (max BP ≈ 0). This is because the minerals with a large surface, such as illite, overshadow the contributions from the quartz in PSR#2. In other words, the surface area of PSR#4 is smaller than PSR#2, where the effect of quartz on the wettability state is more noticeable in PSR#4 compare to PSR#2.

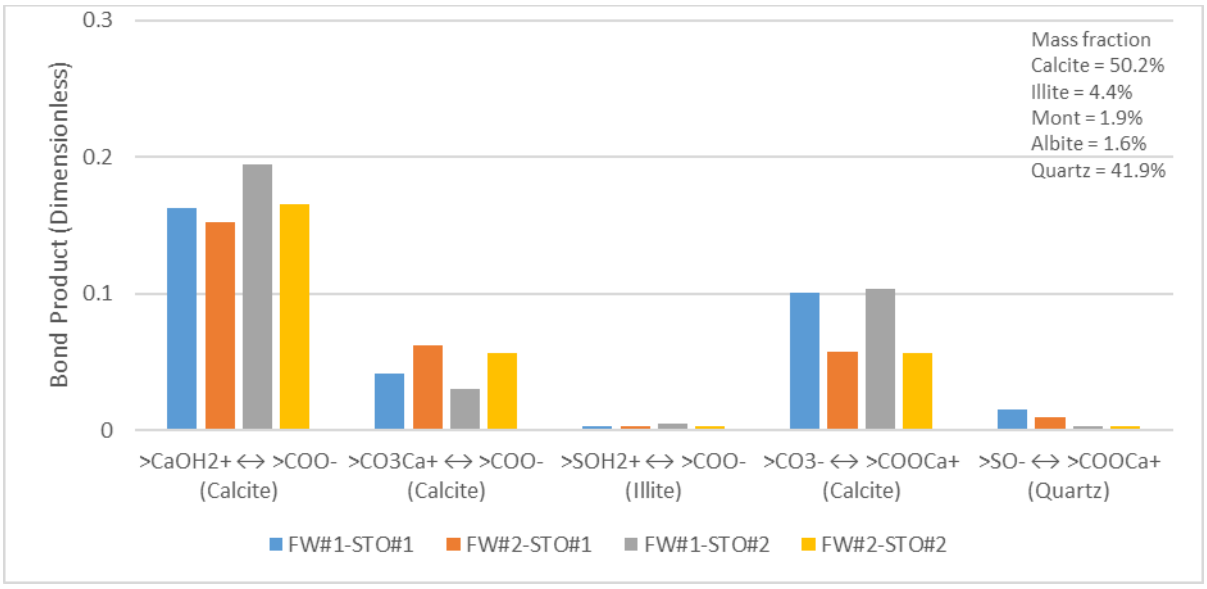

Figure 4. 24: Prediction of the oil-adhesion tendency of PSR#4 using the bond product during FWI.

ii. Carbonated water

During CW injection, the dominant active electrical pair linkage for mineral mixtures (PSR#3 and PSR#4) becomes less hydrophobic (Figure 4.25). This can be explained by the difference between a BP for dominant electrostatic pair linkages before and after applying CW. For example, for PSR#3, the max BP was approximately 0.06 before and 0.03 after CW injection, which led the mineral mixture to act more hydrophilic. Moreover, it can be observed from Figure 4.25 that, after applying CW instead of FW, the dominant electrostatic pair linkage between oil-brine and PSR#3-brine is altered from direct adhesion of carboxylate ($>COO^-$) onto the cationic calcite ($>CaOH_2^+$) surface to direct adhesion of carboxylate ($>COO^-$) onto the cationic illite surface ($>SOH_2^+$).

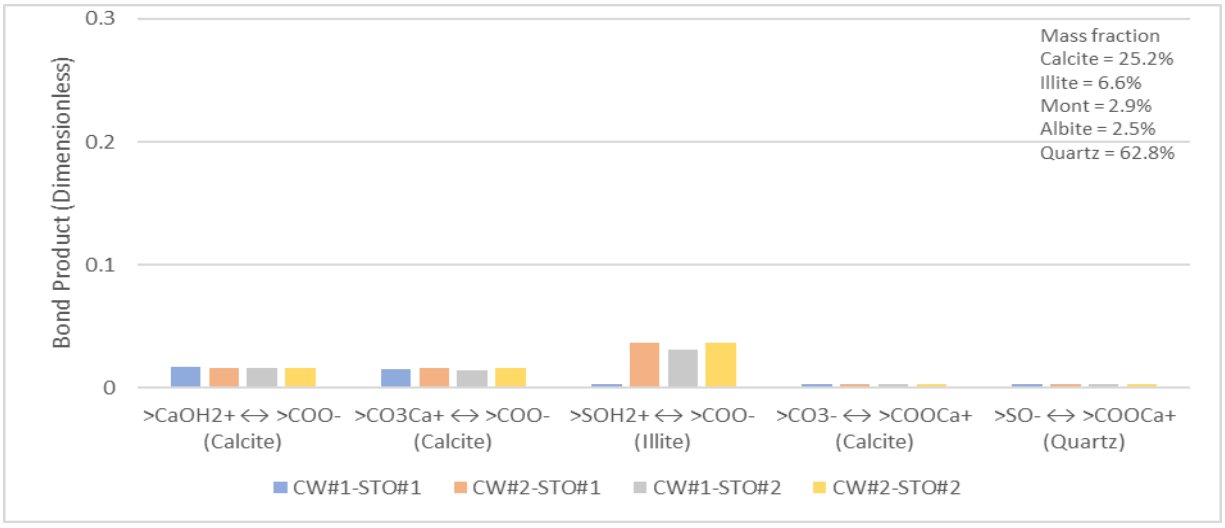

Figure 4. 25: Prediction of the oil-adhesion tendency of PSR#3 using the bond product during CWI.

While in PSR#4, this process can not be observed due to a negligible amount of illite (4.4%) in this mineral mixture. However, like in PSR#3, the wettability preferences of PSR#4 mineral mixture alters from oil-wet to water-wet in CW, proved by decreased BP of the dominant electrostatic pair linkage from 0.2 to 0.07.

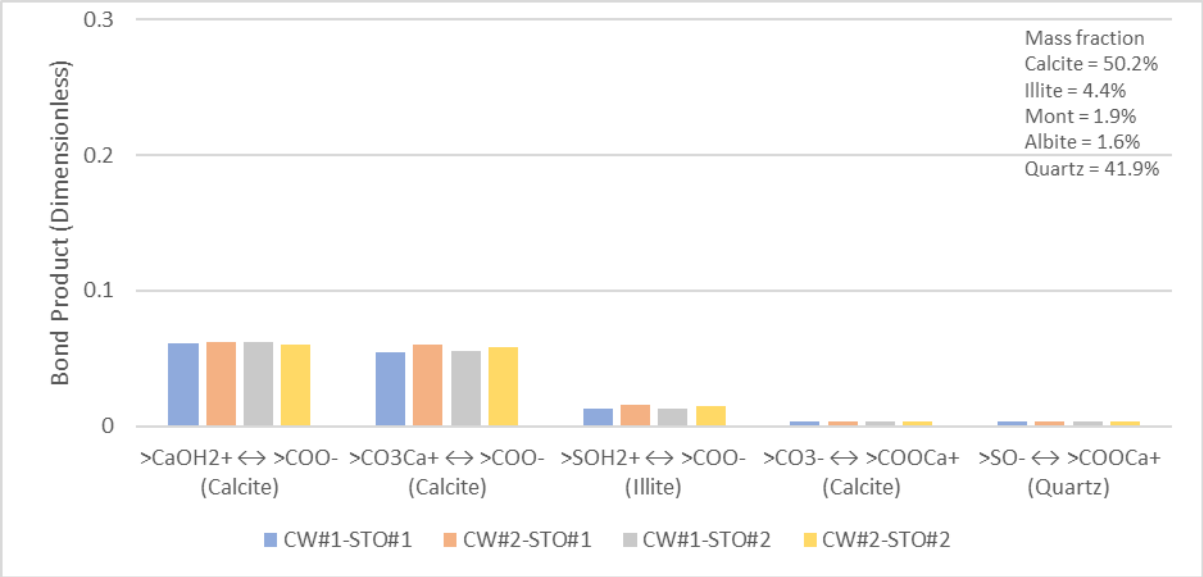

Figure 4. 26: Prediction of the oil-adhesion tendency of PSR#4 using the bond product during CWI.

4.3 Effect of Temperature and Pressure on Calcite Wettability

It is believed that the temperature may remarkably influence the wettability preferences of the rock surfaces, and the pressure dependence is relatively weak [79]–[81]. Some researchers believe that increasing temperature makes it possible to alter wettability toward water-wet [82], [83]. In contrast, other investigators considered that the wettability would alter toward oil-wet rather than water-wet with a temperature rise [84], [85]. Moreover, some scientists assumed that the changes in wettability with the temperature were not just oil-wet or water-wet. For instance, Wang and Gupta [79] and Rao [86] believed that with an increasing temperature, wettability preferences of the sandstone reservoir might alter toward more oil-wet, while in carbonate reservoir, it might alter toward more water-wet.

To better understand the temperature and pressure effect on wettability preferences of individual mineral (calcite), SCM result at different temperatures (60°C, 90°C, and 120°C) and pressures (1bar and 300bar) were compared. Calcite was selected because it is the mineral that has the most significant change in wettability. To accomplish this, the same BP method was used to estimate the wettability preferences of calcite at various reservoir conditions. The results obtained from simulations with FW and CW for different temperatures are presented first to

investigate the alteration of wetting preferences of calcite at various reservoir temperature conditions. Afterward, a similar procedure was done for various reservoir pressure conditions.

4.3.1 Temperature Effect on Calcite Wettability

i. Formation water

Figure 4.27 illustrates the TBP for calcite at reservoir temperatures of 60°C, 90°C, and 120°C during FWI. From SCM results, it can be concluded that the wettability state of calcite is oil-wet at given temperatures, as the TBP number varies from 0.8 to 1 at all three conditions.

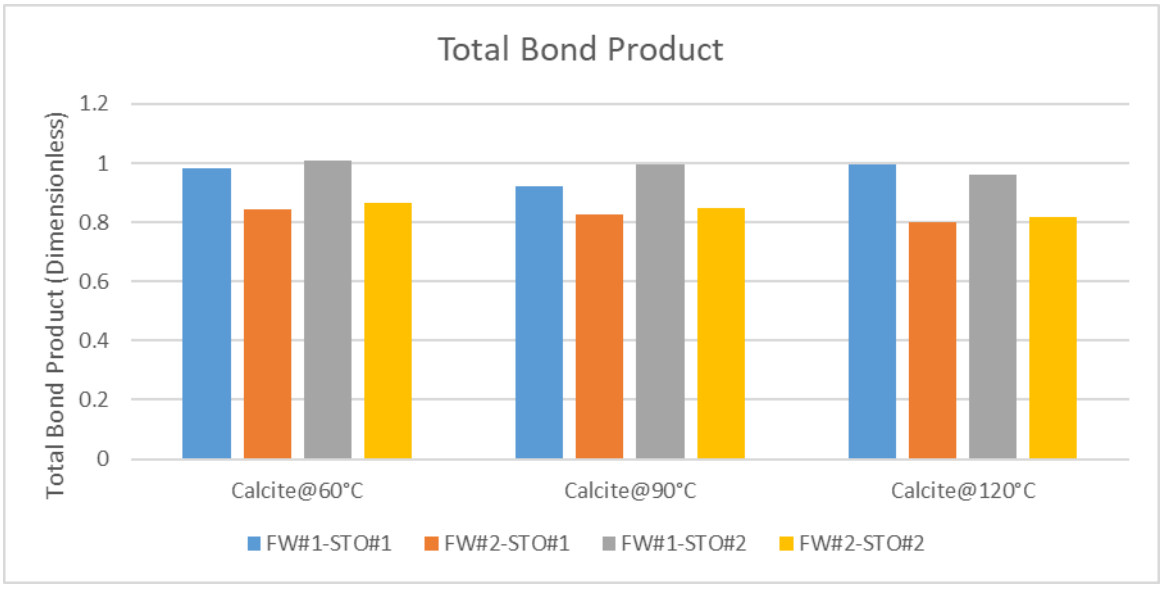

Figure 4. 27: Prediction of the oil-adhesion tendencies of Calcite using the total bond product during FWI in different temperatures.

ii. Carbonated water

A similar effect can be observed after applying CW instead of FW. The results in Figure 4.28 show that given temperatures, calcite wettability is less hydrophobic (TBP < 0.4) in CW than in FW (TBP ≈ 1), as predicted in previous chapters (4.1.1 and 4.1.6). At the same time, the difference in the wetting state of mineral (calcite) at the three reservoir conditions is minimal.

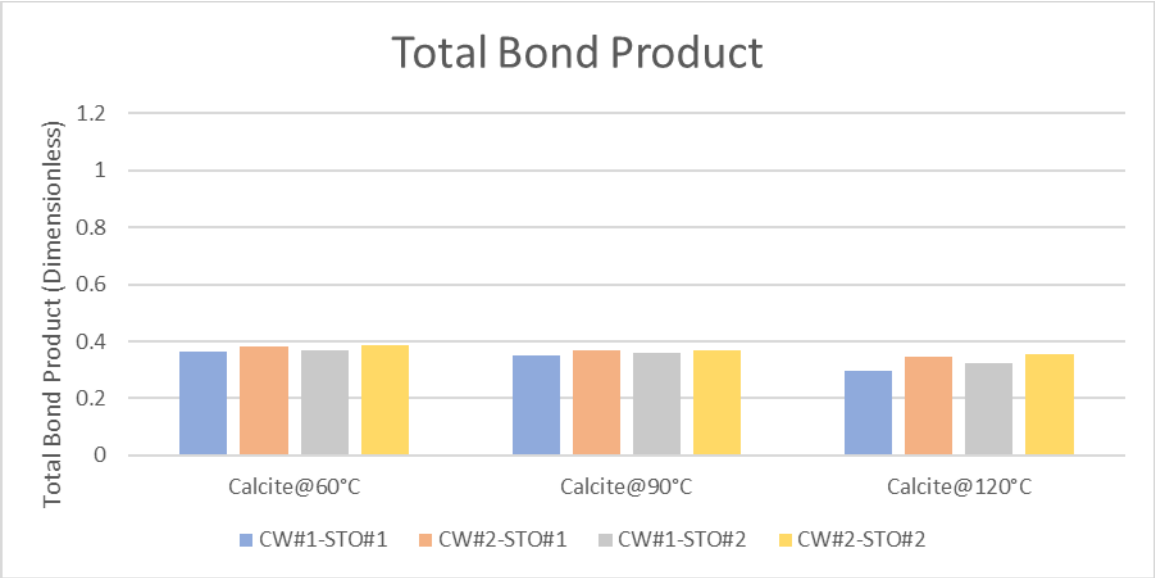

Figure 4. 28: Prediction of the oil-adhesion tendencies of Calcite using the total bond product during CWI in different temperatures.

4.3.2 Pressure Effect on Calcite Wettability

The primary purpose of visualization of the pressure effect on mineral wettability via SCM was to demonstrate how the wetting state of the calcite alters between 1bar and 300 bar. Since all previous simulations with FW were designed for a 1 bar reservoir pressure, while simulations with CW were designed for 300 bar reservoir pressure. From Figure 4.29 and Figure 4.30, it can be concluded that calcite wettability preference is similar at both reservoir pressures and, as predicted before, wettability preferences in FW and CW are oil-wet and less oil-wet, respectively.

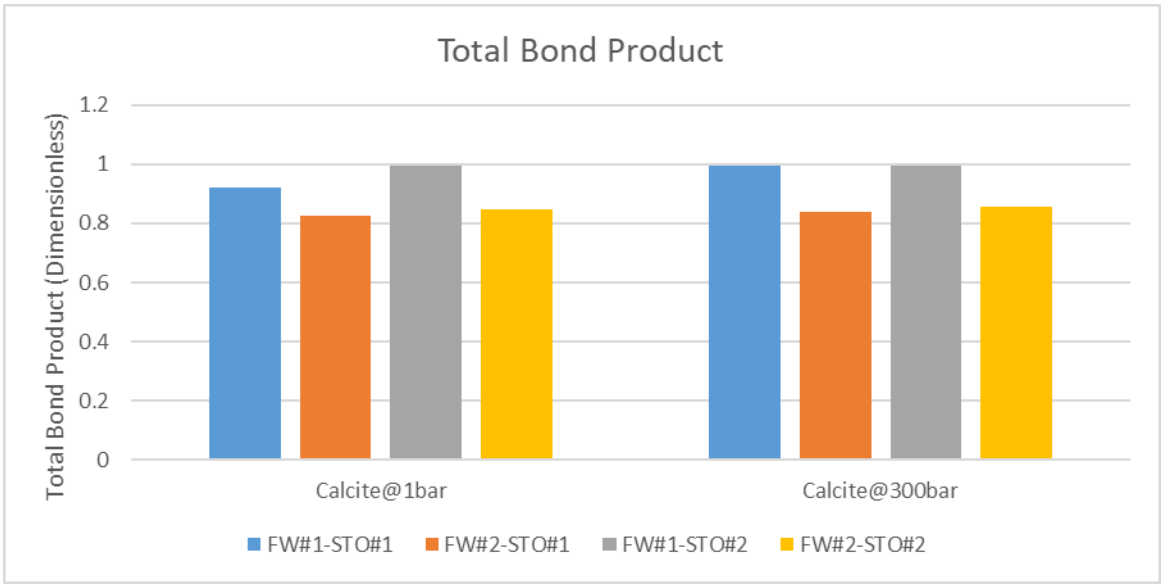

Figure 4. 29: Prediction of the oil-adhesion tendencies of Calcite using the total bond product during FWI in different pressures.

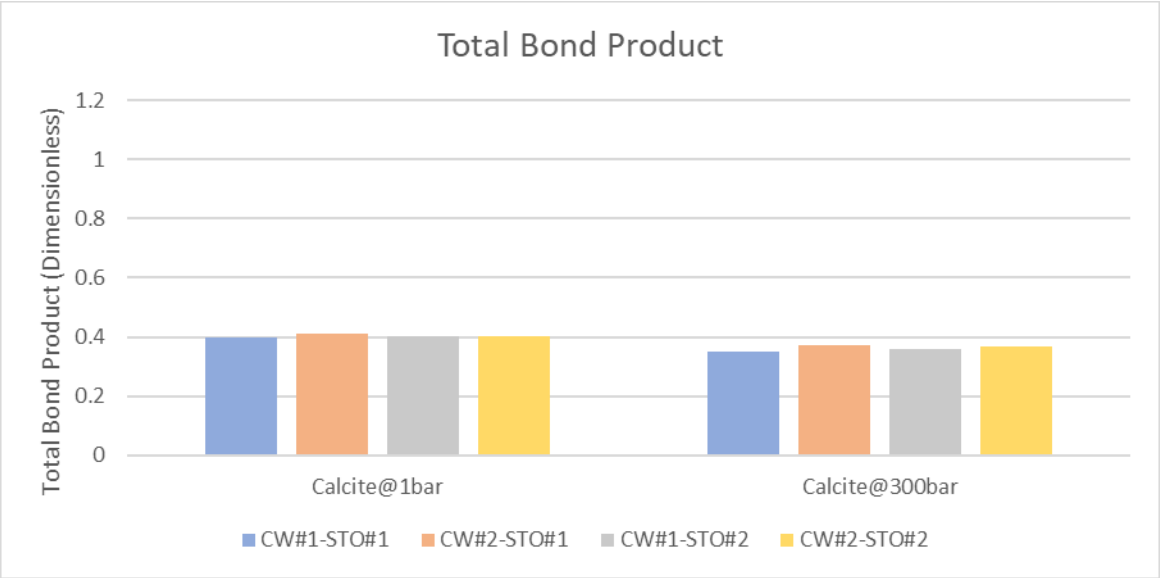

Figure 4. 30: Prediction of the oil-adhesion tendencies of Calcite using the total bond product during CWI in different pressures.

5 Discussion

5.1 Discussion of the Simulation Results and Comparison to Previous Work

5.1.1 Prediction of the Wettability During Formation Water Injection

Simulation results for minerals, reservoir rocks, and mineral mixtures during FWI predicted their wettability preferences based on the attractive electrostatic forces between the oil-brine and the rock-brine interfaces result in the oil adhesion defined by BP. The results show that wettability preferences of quartz and albite were toward water-wet while calcite wetting state was strong oil-wet. On the other hand, wettability preferences of clay minerals such as illite and montmorillonite in FW were intermediate-wet. In other words, the increasing order of the mineral hydrophobicity is given as quartz < albite < illite < montmorillonite < calcite. These minerals were dominant in the sandstone reservoir rocks and mineral mixtures that were investigated in this study. The SCM results show that the wettability preferences of rocks were dictated by the surface area and wetting state of the individual minerals. Above mentioned results match the experimental and simulation results of Erzuah et al. [64]. Moreover, the wettability preferences of the quartz and SRRs are in accordance with the results of Zhang et al. [62], who investigated the wettability preferences of the sandstone rocks and their mineral components before and after CO_2 injection using the captive bubble method.

5.1.2 Prediction of the Wettability During Carbonated Water Injection

In the next step, the wettability preferences of the same minerals, SRRS, and mineral mixtures were predicted after applying CW instead of FW. The primary purpose of the investigation was to understand the effect of CW on the wetting state of the reservoir. From the results, it can be observed that the wettability preferences of the quartz and albite altered toward more water-wet during CWI. However, the same effect was not noticed on clay minerals. The wetting state of illite and montmorillonite changed toward slightly more water-wet and more oil-wet after applying CW, respectively. The sharp change in wetting state during CWI was observed in calcite. Wettability of calcite altered from strongly oil-wet toward intermediate-wet or slightly water-wet. These observations are in accordance with the experimental results of Fjelde et al. [61], in which the COBR interactions during imbibition experiments were investigated. In research, the effect of CO_2 on the wettability of the chalk reservoir was studied where the dominant mineral was calcite.

The wettability preferences of the reservoir rocks (SRR#1 and SRR#2) and mineral mixtures (PSR#1, PSR#2, PSR#3, PSR#4) were altered individually for each rock and mineral mixture

during CWI. As in FWI, wettability preferences of the rocks were dictated by the surface area and wetting state of the individual minerals in CW. The SCM results are in accordance with Fjelde et al. [61] results, in which core experiments were performed for visualization wettability alteration of chalk reservoir during CO_2-WAG. The results are also in accordance with the results of core flooding experiments performed by Al-Mutairi et al. [6], in which they concluded that CWI into carbonate rock causes alteration of the rock wettability from an oil-wet to an intermediate-wet state and increasing CO_2 concentration in the brine leads to more alteration of wetting state.

5.1.3 Prediction of the Effect of Temperature and Pressure on Wettability

From the SCM results, it was concluded that the wettability preference of the calcite is oil-wet in FW, while it alters toward more water-wet. However, SCM results at different temperatures and pressures show that these reservoir properties have minimal effect on the wetting state of calcite in both FW and CW. The results also coincide with the results of experiments performed by Zhang et al. [63], in which the influence of the temperature and pressure on the wettability in COBR systems was investigated by using a captive droplet method. Zhang et al. [63] concluded that pressure from 10 to 70 MPa has no discernible effect on wettability, regardless of the mineral type. However, the temperature had a notable impact on water-wet mineral surfaces, while for neutral-wet or oil-wet samples, the influence of the temperature on wettability was relatively weak.

5.2 Limitations

There were several limitations in SCM results in which wettability was characterized by a geochemical simulator PHREEQ-C. Some of them listed below:

i. Electrostatic pair linkages

In SCM results, wettability preferences were predicted based on the attractive electrostatic forces between the oil-brine and the rock-brine interfaces result in the oil adhesion defined by BP. However, only dominant attractive electrostatic pair linkages were utilized in BP, and non-dominant pair linkages were not considered in the present study. However, it had a minor effect on the SCM results.

ii. Pressure

The experimental background of the present study was flotation tests done by Erzuah et al. [64] in which wettability preferences of the individual minerals and reservoir rocks were determined at pressure 1 bar during FWI. While the results in Chapter 4.3.2 demonstrated that pressure had a minor effect on the wettability preferences of the minerals, consequently on the wettability preferences of the rocks also.

iii. Mineral Distribution

Another limitation in the SCM results was not considering the effect of the mineral distribution. This is because the SCM method predicts wettability by assuming that all mineral surfaces are ready for the reaction. Nevertheless, a possible solution can be decreasing the effective surface area of the individual minerals in simulations. More information about the effective surface area is given in Chapter 5.3

iv. Surface Precipitation

The impact of the surface precipitation was not considered in the SCM results for the reservoirs with asphaltene and wax precipitation. Commonly, crude oils alter their ability to act as solvents for polar components. If oil becomes a poor solvent for asphaltene, it can contribute to a less water-wet condition in the reservoir rock [27] since surface precipitation has an essential role in the wettability estimation of the rock/mineral.

5.3 Proposal of Further Work

As a continuation of the simulation work performed in the present study, I will suggest performing experiments with FW and CW using the USBM method to estimate the wettability preferences of the minerals and reservoir rocks at various pressures and temperatures since the SCM method and flotation tests have limitations in minerals distribution. On the other hand, in USBM experiments, mineral distribution is taken into account since the USBM method estimates the wettability of the bulk rock while the flotation test estimates the wettability of crushed rock. Moreover, the contact surface area of the mineral-brine and oil-brine interactions during the flotation test is higher than the USBM method since crushed rocks are used in the test. The effective surface area of each mineral should be described to get more accurate results. For example, if 90% of the core sample area is dominated by clay mineral, that may be a dominant mineral in simulations. However, the clay mineral may have minor contact with flowing fluid, making the mineral non-dominant. After estimating the effective surface area of

the individual mineral, which is in contact with flowing fluid, it can be applied to SCM instead of using the total surface area of the mineral. In other words, simulations and experiments should be performed at more relevant reservoir conditions to get more accurate results.

6 Conclusion

The work of the present study has shown that the SCM method can be used for estimating the wettability alteration tendencies of the individual minerals and reservoir rocks during CWI in the geochemical simulator PHREEQ-C with different brines and STOs at different temperatures and pressures.

The SCM technique is a quick and economical method of estimating the wettability of the minerals and reservoir rocks via a geochemical simulator, PHREEQ-C. The main positive side of the SCM method over the other wettability estimations methods (e.g., the Amott and the USBM) is that the SCM technique can estimate the wettability alteration tendencies of the minerals and rocks during CWI. Besides, the SCM can predict the mechanisms that led to oil adhesion, such as cation bridging and direct adhesion of carboxylate ($>COO^-$). In addition, the SCM method can be used in the prediction of laboratory experiments. SCM can be utilized as the initial screening tool to estimate the potential for CW effect on reservoir wettability. Afterward, further evaluation of potential in laboratory experiments and reservoir simulations should be performed.

From SCM results, the increasing order of the dominant minerals hydrophobicity in the studied sandstone reservoirs during FWI is given as quartz < albite < illite < montmorillonite < calcite. After CWI, wettability preferences of the quartz, albite, illite, and calcite altered toward more water-wet. Since the increasing order of mineral hydrophobicity also changed slightly, illite and montmorillonite swapped their places: quartz < albite < montmorillonite < illite < calcite.

The SCM results also showed that the wettability preferences of the SRRs and PSRs depend on the wetting state and effective surface area of the dominant mineral, except for rocks with high calcite content. Thus, it can be concluded that the calcite content significantly impacts the wetting state of the studied sandstone rocks more than that of clay. Moreover, the wettability alteration by CW also depends on the wetting state and effective surface area of the dominant mineral. In other words, the wettability preferences of the rock alter towards the wetting state of the dominant mineral during CWI.

Based on the SCM results, increasing pressure from 1 to 300 bar and temperature from 60°C to 120°C had no noticeable effect on the wetting state of the mineral, regardless of mineral types, in the COBR system.

7 Reference

[1] U. Singh, 'Carbon Capture and Storage: An Effective Way to Mitigate Global Warming', *Curr. Sci.*, vol. 105, no. 7, p. 10, Oct. 2013.

[2] B. Metz, O. Davidson, H. Coninck, M. Loos and L. Meyer "Intergovernmental Panel on Climate Change. Working Group III. - IPCC special report on carbon dioxide capture and storage", *Cambridge University Press*, p. 443, 2005.

[3] M. A. Farhadinia and M. Delshad, 'Modeling and Assessment of Wettability Alteration Processes in Fractured Carbonates using Dual Porosity and Discrete Fracture Approaches', *Soc. Pet. Eng.*, p. 13, Apr. 2010.

[4] A. Alhosani, 'Pore-Scale Characterization of Carbon Dioxide Storage at Immiscible and Near-Miscible Conditions in Altered-Wettability Reservoir Rocks', *Int. J. Greenh. Gas Control*, p. 15, Jan. 2021.

[5] J.Ennis-King, 'Role of Convective Mixing in the Long-Term Storage of Carbon Dioxide in Deep Saline Formations', *SPE J.*, p. 8, May 2005.

[6] S. M. Al-Mutairi, S. A. Abu-Khamsin, T. M. Okasha, S. Aramco, and M. E. Hossain, 'An Experimental Investigation of Wettability Alteration During CO2 Immiscible Flooding', *J. Pet. Sci. Eng.*, vol. 120, pp. 73–77, Aug. 2014, doi: 10.1016/j.petrol.2014.05.008.

[7] M. Mohammed and T. Babadagli, 'Wettability Alteration: A Comprehensive Review of Materials/Methods and Testing the Selected Ones on Heavy-Oil Containing Oil-Wet Systems', *Adv. Colloid Interface Sci.*, vol. 220, pp. 54–77, Jun. 2015, doi: 10.1016/j.cis.2015.02.006.

[8] E. Golabi, F.S. Azad, S.S. Ayatollahi, S.N. Hosseini, and M. Dastanian, 'Experimental Study of Anionic and Cationic Surfactants Effects on Reduce of IFT and Wettability Alteration in Carbonate Rock', *Int J Sci Eng Res*, vol. 3, no. 7, pp. 1–8, Jul. 2012.

[9] J.S. Buckley, K. Takamura, and N.R. Morrow, 'Influence of Electrical Surface Charges on the Wetting Properties of Crude Oils', *SPE Reserv. Eng.*, vol. 4, no. 03, pp. 332–340, Aug. 1989, doi: 10.2118/16964-PA.

[10] G. R. Jerauld and J. J. Rathmell, 'Wettability and Relative Permeability of Prudhoe Bay: A Case Study in Mixed-Wet Reservoirs', *SPE Reserv. Eng.*, vol. 12, no. 01, pp. 58–65, Feb. 1997, doi: 10.2118/28576-PA.

[11] C. C. Agbalaka, A. Y. Dandekar, S. L. Patil, S. Khataniar, and J. Hemsath, 'The Effect Of Wettability On Oil Recovery: A Review', in *SPE Asia Pacific Oil and Gas Conference and Exhibition*, Perth, Australia, Oct. 2008, p. 13. doi: 10.2118/114496-MS.

[12] E. C. Donaldson and W. Alam, *Wettability*. Elsevier, 2013.

[13] N. Kasiri and A. Bashiri, 'Wettability and Its Effects on Oil Recovery in Fractured and Conventional Reservoirs', *Pet. Sci. Technol.*, vol. 29, no. 13, pp. 1324–1333, May 2011, doi: 10.1080/10916460903515540.

[14] W. G. Anderson, 'Wettability Literature Survey Part 2', *J. Pet. Technol.*, pp. 1246–1262, Oct. 1986.

[15] A. Mirzaei-Paiaman, 'New Methods for Qualitative and Quantitative Determination of Wettability from Relative Permeability Curves: Revisiting Craig's Rules of Thumb and Introducing Lak Wettability Index', *Elsevier Ltd*, p. 15, Aug. 2021, doi: https://doi.org/10.1016/j.fuel.2020.119623.

[16] D. C. Standnes, 'Enhanced Oil Recovery from Oil-Wet Carbonate Rock by Spontaneous Imbibition of Aqueous Surfactant Solutions', p. 130, doi: https://ntnuopen.ntnu.no/ntnu-xmlui/bitstream/handle/11250/231133/121656_FULLTEXT01.pdf?sequence=1

[17] B. Raeesi, N. R. Morrow, and G. Mason, 'Effect of Surface Roughness on Wettability and Displacement Curvature in Tubes of Uniform Cross-Section', *Colloids Surf. Physicochem. Eng. Asp.*, vol. 436, pp. 392–401, Sep. 2013, doi: 10.1016/j.colsurfa.2013.06.034.

[18] J. A. L. Pabón, T. J. M. Pilonieta, L. F. C. Moreno, H. B. Lombana, J. F. Zapata, and C. A. D. Prada, 'Experimental Comparison for the Calculation of Rock Wettability Using the Amott-Harvey Method and a New Visual Method', *CTF - Cienc. Tecnol. Futuro*, vol. 5, no. 5, pp. 5–22, Dec. 2014, doi: 10.29047/01225383.30.

[19] W. Abdallah and J. S. Buckley, 'Fundamentals of Wettability', *Oilfield Rev.*, no. 01, p. 18, May 2007.

[20] E.C. Donaldson, R. D. Thomas, and P. B. Lorenz, 'Wettability Determination and Its Effect on Recovery Efficiency', *Soc. Pet. Eng. J.*, vol. 9, no. 01, pp. 13–20, Mar. 1969, doi: 10.2118/2338-PA.

[21] W. G. Anderson, 'Wettability Literature Survey- Part 4: Effects of Wettability on Capillary Pressure', *J. Pet. Technol.*, vol. 39, no. 10, pp. 1283–1300, Oct. 1987, doi: 10.2118/15271-PA.

[22] F. F. Craig, Jr., 'The Reservoir Engineering Aspects of Waterflooding', *Soc. Pet. Eng.*, vol. 2, p. 135, 1971.

[23] R. T. Johansen and H. N. Dunning, *Relative Wetting Tendencies of Crude Oils by Capillarimetric Method*. U.S. Department of the Interior, Bureau of Mines, 1961.

[24] V. Kulinič, 'The Influence of Wettability on Oil Recovery', *AGH Drill. Oil Gas*, vol. 32, no. 3, p. 493, Jan. 2015, doi: 10.7494/drill.2015.32.3.493.

[25] W. G. Anderson, 'Wettability Literature Survey Part 5: The Effects of Wettability on Relative Permeability', *J. Pet. Technol.*, vol. 39, no. 11, pp. 1453–1468, Oct. 1987, doi: 10.2118/16323-PA.

[26] Y. Dandekar, *Petroleum Reservoir Rock and Fluid Properties*. CRC Press Taylor & Francis Group, 2006. doi: 10.1201/b15255.

[27] J. S. Buckley, Y. Liu, and S. Monsterleet, 'Mechanisms of Wetting Alteration by Crude Oils', *SPE J.*, vol. 3, no. 01, pp. 54–61, Mar. 1998, doi: 10.2118/37230-PA.

[28] Y. Liu and J. S. Buckley, 'Evolution of Wetting Alteration by Adsorption from Crude Oil', *SPE Form. Eval.*, vol. 12, no. 1, p. 7, Mar. 1997.

[29] C. S. Vijapurapu and D. N. Rao, 'Effect of Brine Dilution and Surfactant Concentration on Spreading and Wettability', *Soc. Pet. Eng.*, p. 8, Feb. 2003.

[30] T. Al-Aulaqi, 'Wettability Alteration by Brine Salinity and Temperature in Reservoir Cores', *Soc. Pet. Eng.*, p. 32, May 2013.

[31] G.Q. Tang and N.R. Morrow, 'Salinity, Temperature, Oil Composition, and Oil Recovery by Waterflooding', *SPE Reserv. Eng.*, vol. 12, no. 04, pp. 269–276, Nov. 1997, doi: 10.2118/36680-PA.

[32] I. Fjelde, S. M. Asen, and A. V. Omekeh, 'Low Salinity Water Flooding Experiments and Interpretation by Simulations', in *SPE Improved Oil Recovery Symposium*, Tulsa, Oklahoma, USA, Apr. 2012, p. 12. doi: 10.2118/154142-MS.

[33] W. G. Anderson, 'Wettability Literature Survey - Part 1: Rock/Oil/Brine Interactions and the Effects of Core Handling on Wettability', *J. Pet. Technol.*, vol. 38:11, pp. 1125–1144, Oct. 1986, doi: https://doi.org/10.2118/13932-PA.

[34] L.E. Treiber and W.W. Owens, 'A Laboratory Evaluation of the Wettability of Fifty Oil-Producing Reservoirs', *Soc. Pet. Eng. J.*, vol. 12, no. 06, pp. 531–540, Dec. 1972, doi: 10.2118/3526-PA.

[35] V. C. George and T. F. Yen, 'Some Notes on Wettability and Relative Permeabilities of Carbonate Reservoir Rocks, II', *Energy Sources*, vol. 7, no. 1, pp. 67–75, Jan. 1983, doi: 10.1080/00908318308908076.

[36] S. Erzuah, I. Fjelde, and A. V. Omekeh, 'Wettability Estimation Using Surface-Complexation Simulations', *SPE Reserv. Eval. Eng.*, vol. 22, no. 02, pp. 509–519, May 2019, doi: 10.2118/185767-PA.

[37] D. L. Parkhurst and T. Appelo, *Description of Input and Examples for PHREEQC Version 3—A Computer Program for Speciation, Batch Reaction, One-Dimensional Transport, and Inverse Geochemical Calculations*. U.S. Geological Survey, Denver, Colorado, 2013.

[38] K. Johnsen, H. Holt, K. Helle and O. K. Sollie, 'Mapping of Potential HSE Issues Related to Large-Scale Capture, Transport and Storage of CO2', *Det Norske Veritas AS*, p. 132, Jan. 2009.

[39] K. Bjorlykke, Ed., *Petroleum Geoscience: From Sedimentary Environments to Rock Physics*, 2nd ed. Berlin Heidelberg: Springer-Verlag, 2015. doi: 10.1007/978-3-642-34132-8.

[40] H. Emami-Meybodi, H. Hassanzadeh, C. P. Green, and J. Ennis-King, 'Convective Dissolution of CO2 in Saline Aquifers: Progress in Modeling and Experiments', *Int. J. Greenh. Gas Control*, vol. 40, pp. 238–266, Sep. 2015, doi: 10.1016/j.ijggc.2015.04.003.

[41] C. Thomas, L. Lemaigre, A. Zalts, A. D'Onofrio, and A. De Wit, 'Experimental Study of CO2 Convective Dissolution: The Effect of Color Indicators', *Int. J. Greenh. Gas Control*, vol. 42, pp. 525–533, Nov. 2015, doi: 10.1016/j.ijggc.2015.09.002.

[42] D. W. Green and G. P. Willhite, *Enhanced Oil Recovery*, Second edition. Richardson, Texas, USA: Society of Petroleum Engineers, 2018.

[43] Primary Recovery | Oilfield Glossary. https://www.glossary.oilfield.slb.com/en/terms/p/primary_recovery.

[44] Secondary Recovery | Oilfield Glossary. https://www.glossary.oilfield.slb.com/en/terms/s/secondary_recovery.

[45] Tertiary Recovery | Oilfield Glossary. https://www.glossary.oilfield.slb.com/en/terms/t/tertiary_recovery.

[46] L. W. Lake, *Enhanced Oil Recovery*. Englewood Cliffs, N.J. : Prentice Hall, 1989. Accessed: Feb. 26, 2021. [Online]. Available: https://www.osti.gov/biblio/5112525

[47] W. C. Lyons, *Working Guide to Reservoir Engineering*. Burlington, Mass.; Oxford: Gulf Professional, 2010.

[48] A. Mandal, 'Chemical Flood Enhanced Oil Recovery: A Review', *Int. J. Oil Gas Coal Technol.*, vol. 9, no. 3, p. 241, Jan. 2015, doi: 10.1504/IJOGCT.2015.069001.

[49] W. Yan and E. H. Stenby, 'The Influence of CO2 Solubility in Brine on CO2 Flooding Simulation', in *All Days*, New Orleans, Louisiana, Oct. 2009, p. SPE-124628-MS. doi: 10.2118/124628-MS.

[50] N. Mungan, 'Carbon Dioxide Flooding - Fundamentals', *Mungan Pet. Consult. Ltd Calg. Alta.*, p. 7, Mar. 1981.

[51] J. G. Speight, ‘Heavy Oil Recovery and Upgrading’, in *Heavy Oil Recovery and Upgrading*, Elsevier, 2019, p. 806. doi: 10.1016/B978-0-12-813025-4.09993-1.

[52] H. J. Haynes, *Enhanced Oil Recovery*. National Petroleum Council; Industry Advisory Council to the U.S. Department of the Interior, 1976.

[53] L. W. Holm and V. A. Josendal, ‘Effect of Oil Composition on Miscible-Type Displacement by Carbon Dioxide’, *Soc. Pet. Eng. J.*, vol. 22, no. 01, pp. 87–98, Feb. 1982, doi: 10.2118/8814-PA.

[54] F.M. Orr and C.M. Jensen, ‘Interpretation of Pressure-Composition Phase Diagrams for CO2/Crude-Oil Systems’, *Soc. Pet. Eng. J.*, vol. 24, no. 05, pp. 485–497, Oct. 1984, doi: 10.2118/11125-PA.

[55] J. P. Heller and J. J. Taber, ‘Influence of Reservoir Depth on Enhanced Oil Recovery by CO2 Flooding’, *Soc. Pet. Eng.*, p. 7, Mar. 1986.

[56] J. J.Sheng, *Enhanced Oil Recovery Field Case Studies*. Gulf Professional Publishing, 2013.

[57] P. M. Jarrell, *Practical aspects of CO2 flooding*. Richardson, Tex: Society of Petroleum Engineers, 2002.

[58] P. B. Lorenz, E. C. Donaldson, and R. D. Thomas, ‘Use of Centrifugal Measurements of Wettability to Predict Oil Recovery’, *Rep Invest - US Bur Mines U. S.*, vol. 7873, Jan. 1974, Accessed: May 04, 2021. [Online]. Available: https://www.osti.gov/biblio/6555725-use-centrifugal-measurements-wettability-predict-oil-recovery

[59] N. R. Morrow, N. Mungan, and Petroleum Recovery Institute, *Wettability and Capillarity in Porous Media*. Calgary, Alberta: Petroleum Recovery Research Institute, 1971.

[60] A.T. Grogan, V.W. Pinczewski, G. J. Ruskauff, and F.M. Orr, ‘Diffusion of CO2 at Reservoir Conditions: Models and Measurements’, *SPE Reserv. Eng.*, vol. 3, no. 01, pp. 93–102, Feb. 1988, doi: 10.2118/14897-PA.

[61] I. Fjelde and S. M. Asen, ‘Wettability Alteration During Water Flooding and Carbon Dioxide Flooding of Reservoir Chalk Rocks’, *Soc. Pet. Eng.*, p. 8, Jun. 2010.

[62] X.Zhang, J. Ge, F. Kamali, F. Othman, Y. Wang, and F. Le-Hussain, ‘Wettability of Sandstone Rocks and their Mineral Components during CO2 Injection in Aquifers: Implications for Fines Migration’, *J. Nat. Gas Sci. Eng.*, vol. 73, p. 103050, Nov. 2019, doi: 10.1016/j.jngse.2019.103050.

[63] Y. Zhang, J. Zeng, J. Qiao, X. Feng, and Y. Dong, 'Investigating the Effect of the Temperature and Pressure on Wettability in Crude Oil–Brine–Rock Systems', *Energy Fuels*, vol. 32, no. 9, pp. 9010–9019, Sep. 2018, doi: 10.1021/acs.energyfuels.8b01404.

[64] S. Erzuah, I. Fjelde, and A. V. Omekeh, 'Effect of Intrinsic Properties of Reservoir Minerals on Wettability via Surface Complexation Modelling', p. 19, doi: 10.2118/185767-PA.

[65] P. Mwangi, G. Thyne, and D. Rao, 'Extensive Experimental Wettability Study in Sandstone and Carbonate-Oil-Brine Systems: Part 1 – Screening Tool Development', *Int. Symp. Soc. Core Anal.*, p. 6, Sep. 2013.

[66] S. Erzuah, I. Fjelde, and A. V. Omekeh, 'Wettability Characterization Using the Flotation Technique Coupled with Geochemical Simulation', Apr. 2017, vol. 2017, no. 1, pp. 1–13. doi: 10.3997/2214-4609.201700309.

[67] S.T. Dubey and P.H. Doe, 'Base Number and Wetting Properties of Crude Oils', *SPE Reserv. Eng.*, vol. 8, no. 03, pp. 195–200, Aug. 1993, doi: 10.2118/22598-PA.

[68] S. Goldberg, 'Surface Complexation Modelling', in *Encyclopedia of Soils in the Environment*, D. Hillel, Ed. Oxford: Elsevier, 2005, pp. 97–108. doi: 10.1016/B0-12-348530-4/00558-0.

[69] P. V. Brady, N. R. Morrow, A. Fogden, V. Deniz, N. Loahardjo, and Winoto, 'Electrostatics and the Low Salinity Effect in Sandstone Reservoirs', *Energy Fuels*, vol. 29, no. 2, pp. 666–677, Feb. 2015, doi: 10.1021/ef502474a.

[70] P. V. Brady, J. L. Krumhansl, and P. E. Mariner, 'Surface Complexation Modeling for Improved Oil Recovery', in *SPE Improved Oil Recovery Symposium*, Tulsa, Oklahoma, Apr. 2012, p. 10. doi: 10.2118/153744-MS.

[71] D. A. Sverjensky and N. Sahai, 'Theoretical Prediction of Single-Site Surface-Protonation Equilibrium Constants For Oxides and Silicates in Water', *Geochim. Cosmochim. Acta*, vol. 60, no. 20, pp. 3773–3797, Oct. 1996, doi: 10.1016/0016-7037(96)00207-4.

[72] D. A. Sverjensky and N. Sahai, 'Theoretical Prediction of Single-Site Surface-Protonation Equilibrium Constants For Oxides and Silicates in Water', *Geochim. Cosmochim. Acta*, vol. 62, no. 23–24, pp. 3703–3716, Dec. 1998, doi: 10.1016/S0016-7037(98)00262-2.

[73] X. Gu and L. Evans, 'Modelling the Adsorption of Cd(II), Cu(II), Ni(II), Pb(II), and Zn(II) onto Fithian Illite', *J. Colloid Interface Sci.*, vol. 307, pp. 317–25, Apr. 2007, doi: 10.1016/j.jcis.2006.11.022.

[74] E. Wieland, H. Wanner, Y. Albinsson, P. Wersin, and O. Kärnland, 'A Surface Chemical Model of the Bentonite-Water Interface and its Implications for Modelling the Near Field

Chemistry in a Repository for Spent Fuel', *Swed. Nucl. Fuel Waste Manag. Co Stockh. Swed.*, p. 78, Jul. 1994.

[75] M. L. Hjuler and I. L. Fabricius, 'Engineering Properties of Chalk Related to Diagenetic Variations of Upper Cretaceous Onshore and Offshore Chalk in the North Sea area', *J. Pet. Sci. Eng.*, vol. 68, no. 3, pp. 151–170, Oct. 2009, doi: 10.1016/j.petrol.2009.06.005.

[76] M. Wolthers, L. Charlet, and P. V. Cappellen, 'The Surface Chemistry of Divalent Metal Carbonate Minerals; A Critical Assessment of Surface Charge and Potential Data Using the Charge Distribution Multi-Site Ion Complexation Model', *Am. J. Sci.*, vol. 308, no. 8, pp. 905–941, Oct. 2008, doi: 10.2475/08.2008.02.

[77] P. V. Cappellen, L. Charlet, W. Stumm, and P. Wersin, 'A surface Complexation Model of the Carbonate Mineral-Aqueous Solution Interface', *Geochim. Cosmochim. Acta*, vol. 57, no. 15, pp. 3505–3518, Aug. 1993, doi: 10.1016/0016-7037(93)90135-J.

[78] D. L. Parkhurst and C. Appelo, *Description of Input and Examples for PHREEQC Version 3—A Computer Program for Speciation, Batch Reaction, One-Dimensional Transport, and Inverse Geochemical Calculations*. U.S. Geological Survey, Denver, Colorado, 2013.

[79] W. Wang and A. Gupta, 'Investigation of the Effect of Temperature and Pressure on Wettability Using Modified Pendant Drop Method', in *SPE Annual Technical Conference and Exhibition*, Dallas, USA, Oct. 1995, p. 10. doi: 10.2118/30544-MS.

[80] Y. Lu, N. F. Najafabadi, and A. Firoozabadi, 'Effect of Temperature on Wettability of Oil/Brine/Rock Systems', *Energy Fuels*, vol. 31, no. 5, pp. 4989–4995, May 2017, doi: 10.1021/acs.energyfuels.7b00370.

[81] O.S. Hjelmeland and L.E. Larrondo, 'Experimental Investigation of the Effects of Temperature, Pressure, and Crude Oil Composition on Interfacial Properties', *SPE Reserv. Eng.*, vol. 1, no. 04, pp. 321–328, Jul. 1986, doi: 10.2118/12124-PA.

[82] F.G. McCaffery and D.W. Bennion, 'The Effect Of Wettability On Two-Phase Relative Penneabilities', *J. Can. Pet. Technol.*, vol. 13, no. 04, Oct. 1974, doi: 10.2118/74-04-04.

[83] S.W. Poston, S. Ysrael, A.K.M.S. Hossain, and E.F., III Montgomery, 'The Effect of Temperature on Irreducible Water Saturation and Relative Permeability of Unconsolidated Sands', *Soc. Pet. Eng. J.*, vol. 10, no. 02, pp. 171–180, Jun. 1970, doi: 10.2118/1897-PA.

[84] R. A. Nasralla and H. A. Nasr-El-Din, 'Impact of Cation Type and Concentration in Injected Brine on Oil Recovery in Sandstone Reservoirs', *J. Pet. Sci. Eng.*, vol. 122, pp. 384–395, Oct. 2014, doi: 10.1016/j.petrol.2014.07.038.

[85] J. Modaresghazani, R. G. Moore, S. A. Mehta, and M. G. Ursenbach, 'Experimental Evaluation of the Effect of Temperature on Wettability of the Grosmont Carbonate Reservoir in Alberta', Jun. 2016, p. 12. doi: 10.2118/180706-MS.

[86] D. N. Rao, 'Wettability Effects in Thermal Recovery Operations', *SPE Reserv. Eval. Eng.*, vol. 2, no. 05, pp. 420–430, Oct. 1999, doi: 10.2118/57897-PA.